

Aus der Universitätsklinik und Poliklinik für Innere Medizin III des  
Universitätsklinikums Halle (Saale)

(Direktor: Prof. Dr. med. Karl Werdan)

## **Directed expression of dominant-negative p73 in mouse hearts**

Dissertation

zur Erlangung des akademischen Grades

Doktor rerum medicarum (Dr. rer. medic) für das Fachgebiet

Physiologie und Pathophysiologie

vorgelegt

der Medizinischen Fakultät

der Martin-Luther-Universität Halle-Wittenberg

von Ying Zhang

geboren am 27.03.1979 in Jiangsu, VR China

Gutachter/Gutachterin:

1. Prof. Dr. Rüdiger Horstkorte
2. PD. Dr. Henning Ebel
3. Prof. Dr. Gerhild Euler

Eröffnungsdatum des Promotionsverfahrens: 05.10.2011

Datum der öffentlichen Verteidigung: 05.04.2012

## Referat

Herzmuskelzellen von Säugetieren verlieren in der Perinatalzeit die Fähigkeit zu Proliferation und Zellteilung. In der Vergangenheit konnte gezeigt werden, dass bei der Aufrechterhaltung dieser kardiomyozytären Zellzyklus-Blockade p53 eine wichtige Rolle spielt. p53 stellt jedoch einen typischen Tumor-Suppressor dar, so dass die p53-Hemmung mit dem Risiko der Tumor-Induktion verbunden ist. p73 stellt ein Mitglied der p53-Familie dar, das in struktureller und funktioneller Hinsicht p53 sehr ähnlich ist. Im Gegensatz zu p53 stellt p73 keinen typischen Tumor-Suppressor dar. Es konnte gezeigt werden, dass die Expression einer dominant-negativen Isoform von p73 (p73DD) die p53/p73-Signalkaskade inhibiert.

Im Rahmen der hier vorgestellten Untersuchung wurde untersucht, inwiefern die Expression von p73DD den Wiedereintritt von Kardiomyozyten in den Zellzyklus ermöglicht. Zur Expression von p73DD wurden rekombinante Adenoviren konstruiert. Mittels der viralen Vektoren wurde p73DD in neonatalen Herzen von Mäusen exprimiert. Die Expression von p73DD resultierte bei den Tieren nach 3 und 14 Tagen in einem signifikanten Anstieg der relativen Herzgewichte. p73DD führte zur vermehrten Proliferation von Kardiomyozyten (BrdU-Inkorporation, Phosphorylierung von Histon3, Expression von AuroraB). Die Proliferation war nicht von vermehrten Kardiomyozyten-Apoptosen begleitet. Als molekularer Mechanismus der Proliferationssteigerung lässt sich die Hemmung des p53-abhängig CDK-Inhibitors p21WAF bei gleichzeitiger Induktion von D-Cyclinen, Cyclin A, B2 und E nachweisen. Des Weiteren zeigte sich, dass p73DD auch zur Proliferation von adulten Kardiomyozyten führt.

p73DD könnte somit einen viel versprechenden Kandidaten zur Stimulation der Proliferation von Kardiomyozyten im Rahmen regenerativer Therapieansätze darstellen.

Zhang, Ying: Directed expression of dominant-negative p73 in mouse hearts. Halle (Saale), Univ., Med. Fak., Diss., 66 Seiten, 2011

**Abstract**

Mammalian cardiomyocytes lose their ability to proliferate shortly after birth. Previous studies have demonstrated that p53 plays an important role in maintaining cell cycle arrest of cardiomyocytes, which might account for the inability of human hearts to regenerate after injury, e.g. myocardial infarction. Thus, inhibition of p53 might be a promising strategy to reactivate cell cycle progression in cardiomyocytes although such a concept is limited by the fact that p53 is a well-known tumor suppressor. N-terminal truncated isoforms of the p53-related protein p73 function as antagonists against p53 and p73 during normal development without induction of tumor.

Recombinant adenovirus encoding dominant-interfering p73 (Ad-p73DD) were generated to inhibit p53/p73 signaling in mouse hearts at different stages. The expression of p73DD led to the increase of the relative heart weights after 3 days and 14 days which was accompanied by a significant increase of proliferating cardiomyocytes (BrdU-incorporation, phosphorylation of histone3, expression of AuroraB) without induction of apoptosis. Progression of cardiomyocyte cell cycle went along with a significant downregulation of the p53-dependent CDK-inhibitor p21WAF both on mRNA and protein level. Furthermore, mRNA and protein expression of D-type cyclins and cyclin A, B2 and E were increased after Ad-p73DD injection. The cell cycle reentry of cardiomyocytes was not restricted to neonatal hearts, but was also found in adult hearts 5 days after intramyocardial injection of Ad-p73DD.

Thus, expression of dominant-negative p73 might be utilized to stimulate proliferation of cardiomyocytes to improve cardiac regeneration.

## Table of Contents

<b>1</b>	<b>INTRODUCTION .....</b>	<b>1</b>
1.1	Cardiomyocyte cell cycle .....	1
1.1.1	Mammalian cell cycle.....	1
1.1.2	Cardiomyocyte cell cycle activity .....	3
1.1.3	p53 and cell cycle control.....	4
1.2	Programmed cell death.....	5
1.2.1	Cell death – basic concept .....	5
1.2.2	Apoptosis pathways.....	6
1.2.3	Apoptotic activities of p53 .....	7
1.3	p73 ... ..	8
1.4	Cardiac hypertrophy .....	10
1.4.1	Physiological and pathological hypertrophy .....	10
1.4.2	Chromatin remodelling and hypertrophy .....	11
1.5	Adenoviral expression vectors.....	12
<b>2</b>	<b>AIM OF THE WORK.....</b>	<b>13</b>
<b>3</b>	<b>MATERIALS AND METHODS.....</b>	<b>14</b>
3.1	Materials.....	14
3.1.1	Mice.....	14
3.1.2	Adenoviral expression constructs.....	14
3.1.3	Chemicals .....	15
3.1.4	Buffers and solutions.....	17
3.1.5	Antibodies.....	18
3.1.6	Enzymes.....	19
3.1.7	Kits.....	19

3.1.8	Primers.....	19
3.1.9	Equipments .....	21
3.2	Methods .....	22
3.2.1	Neonatal rat cardiomyocytes preparation .....	22
3.2.2	Analysis of subcellular localization of p73 isoforms .....	22
3.2.3	p53 reporter assay.....	22
3.2.4	Isolation of genomic DNA and genotyping PCR .....	23
3.2.5	Intrathoracic injection.....	24
3.2.6	Intramyocardial injection.....	25
3.2.7	Immunohistochemical staining.....	25
3.2.8	Myocyte cross-sectional area (MCSA) and interstitial collagen fraction (ICF) determination.....	28
3.2.9	Analysis of mRNA expression .....	28
3.2.10	Analysis of protein expression .....	29
3.2.11	Statistical analysis.....	31
<b>4</b>	<b>RESULTS.....</b>	<b>32</b>
4.1	Subcellular localization of p73DD(wt) and p73DD(mut) .....	32
4.2	p53 luciferase reporter assay .....	33
4.3	Regulation of endogenous p53 and p73 after expression of p73DD(wt) .....	34
4.4	Microarray analysis of gene expression after directed expression of p73DD(wt) in neonatal mouse hearts .....	35
4.5	Effects of directed expression of p73DD(wt) on neonatal mouse hearts .....	36
4.5.1	Expression of p73DD proteins in neonatal mouse hearts.....	36
4.5.2	Effects on cardiomyocyte cell cycle activity .....	37
4.5.3	Effects on cell growth of cardiomyocytes .....	40
4.5.4	Effects on cardiomyocyte apoptosis .....	41

4.5.5	mRNA and protein expression of cell cycle related genes after directed expression of p73DD(wt) .....	42
4.6	Effects of directed expression of p73DD(wt) in adult mouse myocardium .....	44
<b>5</b>	<b>DISCUSSION</b> .....	<b>46</b>
5.1	p73DD(wt) inhibits p53/p73-dependent signaling in vitro.....	46
5.2	p73DD(wt) expression promotes cardiomyocyte proliferation in vivo.....	47
5.3	p73DD(wt) induces cardiac hypertrophy in vivo .....	50
5.4	p73DD(wt) expression does not induce cardiomyocyte apoptosis in vivo .....	51
5.5	p73DD(wt) and E2Fs.....	51
5.6	p73DD: the “big brother” of dominant-negative p53-isoforms?.....	52
5.7	Controversial effects from p73DD(wt) and p73DD(mut) treated hearts.....	53
5.8	Perspectives .....	53
<b>6</b>	<b>CONCLUSION</b> .....	<b>54</b>
<b>7</b>	<b>REFERENCES</b> .....	<b>55</b>
<b>8</b>	<b>THESEN</b> .....	<b>65</b>

**Abbreviation**

ANF	atrial natriuretic factor
APAF-1	apoptotic protease activating factor-1
ATP	adenosine 5'-triphosphate
Bax	Bcl-2-associated X protein
BrdU	5-bromo-2'-deoxyuridine
BSA	bovine serum albumin
CDK	cyclin-dependent kinase
CDIs	CDK inhibitor proteins
CM	cardiomyocyte
CPRG	chlorophenol red- $\beta$ -D-galactopyranoside
$^{\circ}$ C	degree centigrade
DAB	3,3'-diaminobenzidine
DEPC	diethyl pyro-carbonate
DMEM	Dulbecco's Modified Eagle Medium
DMSO	dimethyl sulfoxide
DNA	deoxyribonucleic acid
cDNA	complementary DNA
DTT	dithiothreitol
EDTA	ethylenediaminetetraacetic acid
EGFP	enhanced green fluorescence protein
FCS	fetal calf serum
h	hours
H1299	human non-small cell lung carcinoma cell line (p53 knockout)
HBS	HEPES-buffered saline
HEK 293 cell line	human embryonic kidney 293 cell line
i.e.	id est
L	liter
LacZ	$\beta$ -galactosidase
m	milli

## VIII

$\mu$	micro
M	molar (mol/l)
MCSA	myocyte cross-sectional area
min	minutes
n	number
$\alpha$ MHC-nlsLacZ	$\alpha$ myosin heavy chain-nuclear localized LacZ
%	percent
PAGE	polyacrylamide gel electrophoresis
PBS	phosphate-buffered saline
PCR	polymerase chain reaction
PFA	paraformaldehyde
PMSF	phenylmethylsulfonyl fluoride
pRB	retinoblastoma protein
RNA	ribonucleic acid
Rnase	RNA nuclease
RT	room temperature
RT-PCR	reverse transcriptase-polymerase chain reaction
s	second
SDS	sodium dodecyl sulfate
SDS-PAGE	sodium dodecylsulfate polyacrylamide gel electrophoresis
TE	Tris-EDTA buffer
U	unit
X-gal	5-bromo-4-chloro-3-indolyl- $\beta$ -D-galactoside

# 1 INTRODUCTION

## 1.1 Cardiomyocyte cell cycle

### 1.1.1 Mammalian cell cycle

The most basic function of the cell cycle is to duplicate accurately the vast amount of DNA in the chromosomes and then segregate the copies precisely into two genetically identical daughter cells [1]. These processes define the two major phases of the cell cycle. Chromosome duplication occurs during S phase (S for DNA synthesis), which requires 10-12 hours and occupies about half of the cell-cycle time in a typical mammalian cell [2]. After S-phase, chromosome segregation and cell division occur in M phase (M for mitosis), which requires much less time. M phase comprises two major events: nuclear division, or mitosis, during which the copied chromosomes are distributed into a pair of daughter nuclei; and cytoplasmic division, or cytokinesis, when the cell itself divides in two [3].

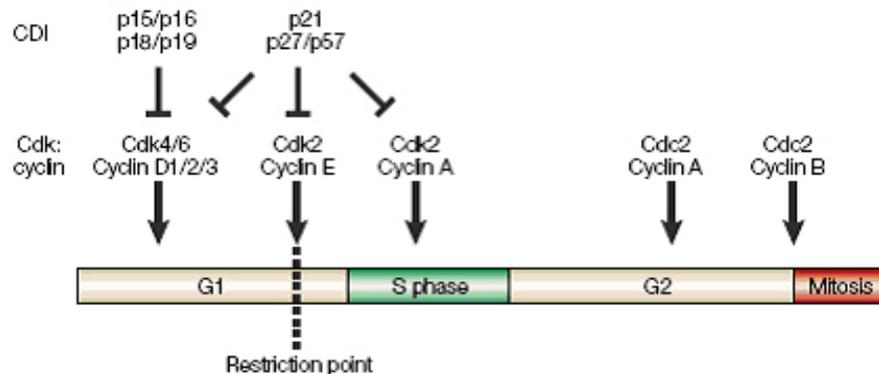


**Figure 1: The mammalian cell cycle [4].** The cell-division cycle is usually divided into four distinct phases and the cell-cycle progression is controlled by the sequential activation of the cyclin-dependent kinases. CDK: cyclin-dependent kinase, CDI: CDK inhibitor, G1: gap1, S phase: DNA synthesis phase, G2: gap2, M phase: mitosis.

At the end of S phase, the DNA molecules in each pair of duplicated chromosomes are intertwined and held tightly together by specialized protein linkages. Early in mitosis at

a stage called prophase, the two DNA molecules are gradually disentangled and condensed into pairs of rigid and compact rods called sister chromatids, which remain linked together by sister-chromatid cohesion. When the nuclear envelope disassembles later in mitosis, the sister chromatid pairs become attached to the mitotic spindle, a giant bipolar array of microtubules. Sister chromatids are attached to opposite poles of the spindle, and, eventually, all sisters align at the spindle equator in a stage called metaphase. The destruction of sister-chromatid cohesion at the start of anaphase separated the sister chromatids, which are pulled to opposite poles of the spindle. The spindle is then disassembled, and the segregated chromosomes are packaged into separate nuclei at telophase. Cytokinesis then cleaves the cell in two, so that each daughter cell inherits one of the two nuclei [3].

Partly to allow more time for growth, most cell cycles have extra gap phases – a G1 phase between M phase and S phase and a G2 phase between S phase and mitosis. Thus, the eukaryotic cell cycle is traditionally divided into four sequential phases: G1, S, G2, and M. G1, S, and G2 together are called interphase [2].

The two gap phases also provide time for the cell to monitor the internal and external environment to ensure that conditions are suitable and preparations are complete before the cell commits itself to the major upheavals of S phase and mitosis. If extracellular conditions are favourable and signals to grow and divide are present, cells in early G1 or G0 progress through a commitment point near the end of G1 known as the restriction point [5]. After passing this point, cells are committed to DNA replication, even if the extracellular signals that stimulate cell growth and division are removed.

In most eukaryotic cells, the cell-cycle control system triggers cell-cycle progression at three major regulatory transitions, or checkpoints [6]. The first checkpoint is Start in late G1, where the cell commits to cell-cycle entry and chromosome duplication. The second is the G2/M checkpoint, where the control system triggers the early mitotic events that lead to chromosome alignment on the spindle in metaphase. The third is the metaphase-to-anaphase transition, where the control system stimulates sister-chromatid separation, leading to the completion of mitosis and cytokinesis. The control system blocks progression through each of these checkpoints if it detects problems inside or outside the cell [5].

Central components of the cell-cycle control system are members of a family of protein kinases known as cyclin-dependent kinases (CDKs) [7]. The activities of these kinases rise and fall as the cell progresses through the cycle, leading to cyclical changes in the

phosphorylation of intracellular proteins that initiate or regulate the major events of the cell cycle.

Cyclical changes in CDK activity are controlled by a complex array of enzymes and other proteins that regulate these kinases [8]. The most important of these CDK regulators are proteins known as cyclins. CDKs, as their name implies, are dependent on cyclins for their activity: unless they are tightly bound to a cyclin, they have nearly no protein kinase activity [9]. Cyclins were originally named because they undergo a cycle of synthesis and degradation in each cell cycle. Cyclical changes in cyclin protein levels result in the cyclic assembly and activation of the cyclin-CDK complexes, this activation in turn triggers cell-cycle events. The initial commitment to a new round of cell division requires transit through restriction point (G1 to S), regulated by CDK4/6 and the D-type cyclins [10]. CDK4/cyclin D-mediated phosphorylation of members of the Rb protein family disrupts Rb-E2F binding, thereby permitting E2F-mediated transcription of genes involved in regulating DNA synthesis [11]. After the restriction point, the CDK/cyclin D activity is no longer required for the cell cycle progression. Cyclin E activates CDK2 during the G1/S phase transition [12]. Cyclin A binds to CDK2 during S-phase or to CDC2 in the G2/M phase transition [12]. The cyclin B/CDC2 complex also functions during the G2/M phase transition [7].

The activity of CDK complexes is also negatively regulated by the CDK-inhibitory subunits – CKIs. In mammalian cells, two classes of CKIs, the Cip/Kip and the Ink4 families, provide a tissue-specific mechanism by which cell cycle progression can be restrained in response to extracellular and intracellular signals [13]. The Cip/Kip family includes p21 [14], p27 [15] and p57 [16] and predominantly inhibits the CDKs of the G1/S-phase transition. The members of INK4 family, comprising p15 [17], p16 [18], p18 [19] and p19 [20], block the progression of the cell cycle by binding to either CDK4 or CDK6 and inhibiting the action of cyclin D.

### **1.1.2 Cardiomyocyte cell cycle activity**

In the adult myocardium, it is generally accepted that the vast majority of cardiomyocytes do not proliferate [21]. This view is supported partially by clinical observations that functionally significant myocardial regeneration has not been documented in diseases and/or injuries that result in cardiomyocyte loss. Furthermore, primary myocardial tumours are rarely noted in adults. Although some findings suggest

that adult cardiomyocytes retain the proliferative capacity, there is considerable debate regarding the frequency at which cardiomyocyte proliferation occurs and if re-initiation of DNA synthesis necessarily leads to cell division [22, 23].

Previous studies demonstrated that in mice there are two temporally distinct phases of cardiomyocyte DNA synthesis. The first phase of DNA synthesis occurs in fetal life and is associated exclusively with cardiomyocyte proliferation [24]. An exceedingly high level of DNA synthesis (around 70 %) is seen in the precardiac mesoderm of the myoepicardial plate in E8 mouse embryos. The onset of cardiomyogenic differentiation is accompanied by transient reduction in the DNA synthesis that recovers to approximately 45 % by E11 during mouse ontology and the overall rate of cardiomyocyte proliferation gradually declines during later stages of embryogenesis [21]. The second phase occurs in immediate postnatal life. Shortly after birth, there is a transition from hyperplastic to hypertrophic myocardial growth. At the morphological level, this transition is characterized by a marked increase in myofibril density, the appearance of mature intercalated discs, and the formation of binucleated cardiomyocytes [25]. Numerous studies have demonstrated a gradual decrease in DNA synthesis that is coincident with the appearance of binucleated cardiomyocytes, leading to the suggestion that binucleation results from a round of genomic duplication and karyokinesis in the absence of cytokinesis [26, 27].

Many regulatory molecules that control the mammalian cell cycle have recently been identified. In general, positive cell cycle regulators (such as, cyclins, cyclin-dependent kinases [CDKs], and protooncogenes) are highly expressed in the embryonic hearts where the cell cycle activity of cardiomyocytes is relatively high [21]. Most of these positive cell cycle regulators are down regulated in the adult heart. In general, expression patterns of negative cell cycle regulators genes (such as CDK inhibitors) are frequently increased in adult hearts, where cardiomyocyte cell cycle activity is largely absent. However, there are some reports showing that at least under certain pathological conditions some cardiomyocytes re-enter the cell cycle [27].

### **1.1.3 p53 and cell cycle control**

p53 is a short-lived transcription factor that has been most extensively studied in its capacity to mediate innate tumour suppression [28]. In addition, there is evidence that p53 can play a part in determining which response is induced through differential activation of target-gene expression. p53 controls the mammalian cell cycle checkpoint

in response to the DNA damage through activation of the p21 gene, which directly inhibits the activity of CDKs needed for entry into S phase. In accordance, p21 knockout mice exhibit a partial failure to arrest at G1 [29]. Inactivation of p53 (e.g., by SV40 large T-antigen) may extend the life of cells that are of late passage, thereby implicating a role of p53 in cellular senescence. Cells from p53-null mice are able to escape cellular senescence and produce aneuploid immortalized cell lines [30].

In mammalian hearts, p53 is also known to be involved in the regulation of the cardiomyocytes' cell cycle. Induction of cell cycle activity in transgenic animals was achieved by the expression of SV40 large T-antigen oncoprotein [31]. It was believed that the cardiomyocytes proliferation in part might have been resulted from T-antigen binding to endogenous cell cycle regulator proteins. Later three predominant cardiomyocyte T-antigen binding proteins, p53, p107 and p193 were identified. Some other studies further support a central role for p53 in DNA tumour virus oncoprotein-induced cardiomyocyte proliferation. The antagonization of p193 and p53 activity relaxes cell cycle checkpoints that would otherwise prevent reactivation of cardiomyocyte DNA synthesis after injury [32]. The blockade of p53 activity enables border zone cardiomyocytes to re-enter the cell cycle after myocardial infarction, which suggests that p53 induction engages a cardiomyocyte cell cycle checkpoint [32].

## **1.2 Programmed cell death**

### **1.2.1 Cell death – basic concept**

Cells can activate an intracellular death program and kill themselves in a controlled way – a process called programmed cell death or apoptosis. In this way, animal cells that are irreversibly damaged, no longer needed, or are a threat to the organism can be eliminated quickly and neatly. During this process the cells shrink, condense, and frequently fragment, and neighbouring cells or macrophages rapidly phagocytose the cells or fragments before there is any leakage of cytoplasmic contents.

Necrosis is a general term describing another mode of cell death that differs from apoptosis, in which the cells suffer a major insult, resulting in a loss of membrane integrity, swelling and disrapture of the cells [33]. However, dead cells are so severely degraded at the final stage that it cannot be morphologically determined whether they died via apoptosis or necrosis. To address this issue, an old term – “oncosis” – was proposed to substitute “necrosis” in cells dying via a process involving cellular swelling

or dropsy [34]. Necrosis, was then proposed to refer to the final stage of either apoptosis or oncosis.

Autophagic cell death is another form of programmed cell death that was thought to be a physiological process for eliminating unnecessary cells [35]. In contrast to apoptosis, autophagic cell death is caspase-independent, and vacuolar degeneration is its most characteristic feature.

### **1.2.2 Apoptosis pathways**

Apoptosis is an energy dependent process that is tightly regulated and at the same time it is a highly efficient cell death program that requires the interplay of a multitude of factors. The components of the apoptotic signaling network are genetically encoded and are considered to be usually in place in a nucleated cell ready to be activated by a death-inducing stimulus [34].

Cells use at least two distinct pathways to activate initiator procaspases and trigger a caspase cascade leading to apoptosis: the intrinsic pathway is activated by intracellular signals generated when cells are stressed; the extrinsic pathway is activated by extracellular ligands binding to cell-surface death receptors [36]. Each pathway uses its own initiator procaspases, which are activated in distinct activation complexes, called the DISC and the apoptosome, respectively [37].

The intracellular machinery responsible for apoptosis depends on a family of proteases that have a cysteine at their active site and cleave their target proteins at specific aspartic acids. They are therefore called caspases (c for cysteine and asp for aspartic acid). Caspases are synthesized in the cell as inactive precursors, or procaspases, which are typically activated by proteolytic cleavage. Procaspase cleavage occurs at one or two specific aspartic acids and is catalyzed by other caspases; the procaspase is split into a large and a small subunit that form a heterodimer, and two such dimers assemble to form the active tetramer. Once activated, caspases cleave, and thereby activate, other procaspases, resulting in an amplifying proteolytic cascade [38].

Extracellular signal proteins binding to cell-surface death receptors trigger the extrinsic pathway of apoptosis. Death receptors are transmembrane proteins containing an extracellular ligand-binding domain, a single transmembrane domain, and an intracellular death domain, which is required for the receptors to activate the apoptotic program. The receptors are homotrimers and belong to the tumour necrosis factor (TNF) receptor family, which includes a receptor for TNF itself and the Fas death

receptor. The ligands that activate the death receptors are also homotrimers; they are structurally related to one another and belong to the TNF family of signal proteins [39]. A well-understood example of how death receptors trigger the extrinsic pathway of apoptosis is the activation of Fas on the surface of a target cell by Fas ligand on the surface of a killer (cytotoxic) lymphocyte [40]. When activated by the binding of Fas ligand, the death domains on the cytosolic tails of the Fas death receptors recruit intracellular adaptor proteins, which in turn recruit initiator procaspases (procaspase-8, procaspase-10), forming a death-inducing signaling complex (DISC) [41]. Once activated in the DISC, the initiator caspases activate downstream executioner procaspases to induce apoptosis.

### **1.2.3 Apoptotic activities of p53**

One of the most dramatic responses to p53 is the induction of apoptosis [42]. Although p53 has been implicated in both intrinsic and extrinsic pathways, it predominantly seems to influence the intrinsic pathway [43]. The intrinsic pathway leads to a perturbation of mitochondrial membrane potential, and so the release of apoptogenic factors from the mitochondrial intermembrane space into the cytoplasm [43]. A family of proteins with structurally conserved domains, known as the Bcl-2 homology (BH) domains, have a central role in the intrinsic apoptotic pathway [44]. Two of these BH-domain proteins, Bax and Bak, function to promote apoptosis by regulating mitochondrial membrane potential. Anti-apoptotic BH-2 proteins, such as Bcl-2 and Bcl-xL, negatively regulate Bax and Bak, whereas a further group of these proteins, the Bcl-2 homology domain-3 (BH3)-only proteins, control these survival proteins. One of the key contributions of p53 to apoptosis is the induction of the expression of genes that encode apoptotic proteins, functioning in both extrinsic and intrinsic pathways [42]. Many potential apoptotic target genes of p53 have been described, including those that encode the BH3-domain proteins NOXA and PUMA. Deletion of many of the described apoptotic targets of p53 has little effect on the sensitivity of the cell to stress-induced apoptosis, probably reflecting the multitude of the other apoptotic signals that can be induced by p53 [45]. The dramatic effect that loss of PUMA has on the sensitivity of several different cell types to p53-induced cell death is therefore particularly telling, indicating that PUMA is a crucial mediator of apoptosis in response to p53 [46]. Interestingly, PUMA has been proposed to function to release cytoplasmic p53 from

inhibitory interactions with anti-apoptotic BH3-domain proteins, allowing p53 to function in a transcriptionally independent manner as a BH3-only protein [46].

### 1.3 p73

The p53 protein was discovered in 1979 through its physical interactions with transforming proteins of DNA tumour viruses [47]. p53 has evolved, since that time, from a potential oncogene to the principle tumour suppressor in mammals: its inactivation is a precondition to most human cancers [48]. Further confirmation of the role of p53 in tumour suppression has come from animal studies that show increased tumorigenesis in p53-null mice [49, 50].

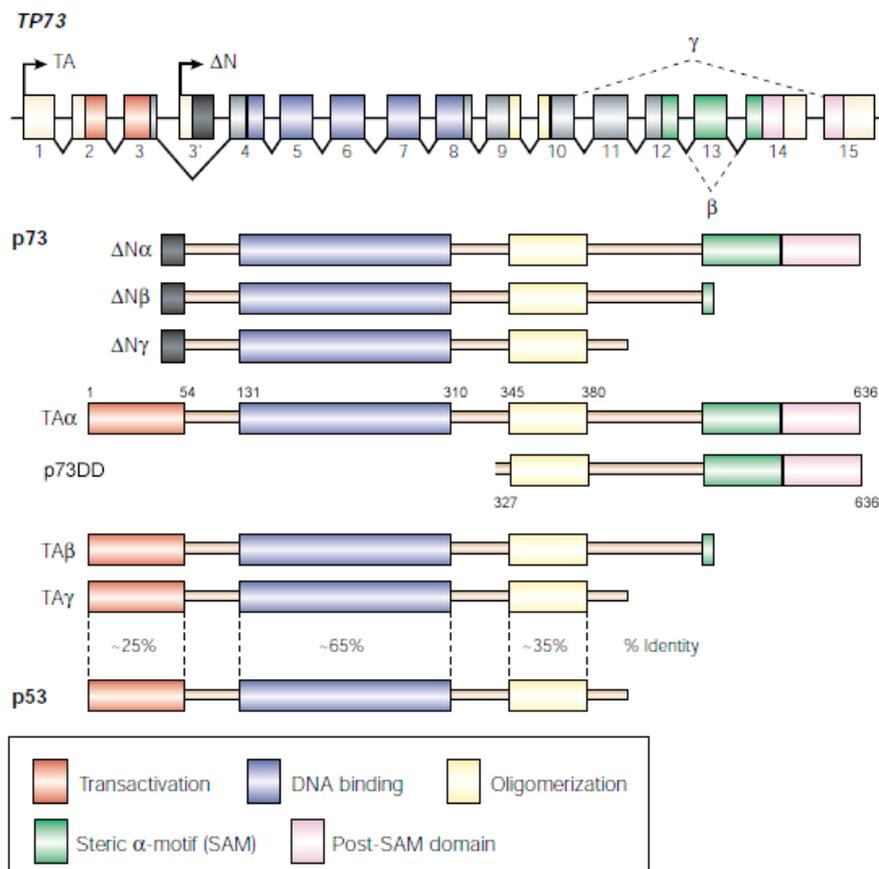


**Figure 2: Gene structure of TP73, TP53 and p73DD (modified) [51].** The TP73 contains two separate promoters give rise to the transactivating (TA) and ΔN classes of product. Alternative splicing at the carboxyl terminus yields further p73 isoforms (e.g., a, b, g). Sequence identity and domain homology to the tumour suppressor TP53 are indicated. p73 mutant (p73DD), encompassing C-terminal portions of p73 (amino acid 327-636), was constructed and exerted dominant-negative effects [52].

p73, a p53-related gene, was identified in 1997 [53]. The p53 and p73 proteins share significant homology both at the genomic and the protein level (Fig. 2). Each of these proteins contains the acidic amino terminal transactivation domain (TAD), the central core specific DNA-binding domain (DBD) and the carboxy-terminal oligomerization domain (OD). Unlike p53 protein, p73 contains long C-termini. The highest level of homology is observed in the DBD (65 % identity between p53 and p73), which suggests that the two proteins can bind to the same DNA sequence and are responsible for transactivation from the same set of promoters [51], causing cell cycle arrest or apoptosis. In addition, p73 shows 25 % identity with the TAD and 35 % identity with OD. Different splicing of the p73 gene is responsible for formation of seven C-terminal p73-isoforms and four N-terminal isoforms. The TP73 gene is alternatively transcribed from two different promoters: P1 in the 5' UTR upstream of a noncoding exon 1, and P2 located within the 23 kb spanning intron 3. P1 and P2 promoters give rise to two different proteins: i) TA-p73 with transactivation domain (TA) and ii)  $\Delta$ N-p73 that lacks the TA domain [51].

Despite the similarities between p53 and p73 activity, it has become evident that they are not functionally redundant. Unlike p53, p73 is not considered as a typical tumour suppressor as it is usually not found mutated in malignancies and mice lacking p73 do not show signs of increased tumour formation [54, 55]. Genetic manipulated mice, which were functionally deficient for all p73 isoforms, exhibited profound developmental defects, including hippocampal dysgenesis, hydrocephalus, chronic infections and inflammation, as well as abnormalities in pheromone sensory pathways [56].

The TAp73 isoforms are able to bind specifically to DNA through p53 response element (RE) and activate transcription of target genes which are responsible for inducing cell cycle arrest and apoptosis [57], however, studies also indicate that p73 proteins can bind DNA through response element slightly different to p53RE [58]. In addition,  $\Delta$ Np73 isoforms were also shown to directly activate specific gene targets not induced by TA isoforms [59].

Previous studies clearly demonstrated that the  $\Delta$ N isoforms of p73 protein can exert dominant-negative effects over p53 and p73 activities by either competing for DNA binding sites or by direct protein interaction [60, 61] [62]. For instance, The  $\Delta$ Np73 isoforms are highly expressed in the developing mouse brain [63] to counteract p53-mediated neuronal death. The removal of the nerve growth factor leads to both an

induction of p53-mediated cell death and a decrease of  $\Delta$ Np73. The importance of  $\Delta$ Np73 in this system is demonstrated by the fact that increasing  $\Delta$ Np73 levels alone rescue the sympathetic neurones from death [63].

In another study, the authors constructed a mutant p73 protein (p73DD(wt)) encompassing C-terminal portions of p73alpha (amino acid 327-636) (Fig. 2), which exerted the dominant-negative effects over p73 and blocked p73-dependent transcriptional activation and apoptosis [52]. These effects were specific as they were not observed using a p73DD mutant which harbours a point mutation (L371P) leading to the loss of the dominant-negative properties (p73DD(mut)).

## **1.4 Cardiac hypertrophy**

### **1.4.1 Physiological and pathological hypertrophy**

Physiological cardiac growth is a feature of normal postnatal development in which an increase in cardiac muscle cell diameter is observed as infants mature to adults.

Insulin or IGF-1 has been proposed to regulate developmental and physiological growth of the heart [64]. Ligand binding to the IGF-1 receptor activates PI3K of the IA group (PI3K $\alpha$ ). PI3K $\alpha$  is a heterodimer that consists of a p85 regulatory subunit and a p110 catalytic subunit. PI3K activation results in the sarcolemmal recruitment of the kinases AKT/PKB and phosphoinositide-dependent kinase-1 (PDK-1) through their pleckstrin-homology domains. When PDK-1 and AKT/PKB are brought into close proximity, PKD-1 phosphorylates and thereby activates AKT/PKB [65]. Of the three AKT genes, only AKT1 and AKT2 are highly expressed in the heart [66, 67]. AKT1 knockout (AKT1 $^{-/-}$ ) mice have a 20 % reduction in body size, with a concomitant reduction in heart size [66]. More recently, AKT1 $^{-/-}$  mice were also shown to be defective in exercise-induced cardiac hypertrophy [66]. These findings indicated that AKT/PKB signaling is indeed important for the physiological growth of the heart. GSK3 $\beta$ , which is normally active but becomes inhibited by AKT/PKB-mediated phosphorylation, is an important downstream target of AKT/PKB in the heart [68]. Active GSK3 $\beta$  negatively regulates hypertrophic transcriptional effectors, such as  $\beta$ -catenin.  $\beta$ -catenin is a cytoplasmic structural protein that can translocate to the nucleus and induce gene expression through binding to transcription factors. The overexpression of active GSK3 $\beta$  in the heart blunted hypertrophy in response to pressure overload, or  $\beta$ -adrenergic stimulation, respectively [68].

In contrast, pathological hypertrophy which regularly occurs in patients with hypertension or valvular heart disease, shows a number of molecular distinctions from physiological hypertrophy. For example, pathological cardiac hypertrophy is typically associated with interstitial fibrosis, activation of a fetal gene program, and myocyte apoptosis [69], whereas physiological heart growth does not display these features.

Cardiac myocytes are normally surrounded by a fine network of collagen fibers. In response to pathological stress (for instance after MI), cardiac fibroblasts secrete extracellular matrix proteins disproportionately and excessively. Myocardial fibrosis, a characteristic of many forms of cardiac pathology, leads to mechanical stiffness of the myocardium, which contributes to contractile dysfunction [70].

As mentioned above, another hallmark of pathological hypertrophy is the reactivation of a set of fetal cardiac genes, including those encoding atrial natriuretic peptide, B-type natriuretic peptide, and fetal isoforms of contractile proteins, such as skeletal  $\alpha$ -actin and  $\beta$ -myosin heavy chain ( $\beta$ -MHC) [71]. These genes are typically repressed postnatally and replaced by the expression of a set of adult cardiac genes. The consequences of fetal gene expression on cardiac function and remodeling are not completely understood, but the upregulation of  $\beta$ -MHC, a slow ATPase, and downregulation of  $\alpha$ -MHC, a fast contracting ATPase, in response to stress has been implicated in the diminution of cardiac function. Relatively minor changes in the ratio of  $\alpha$ - to  $\beta$ -MHC have been shown to have profound effects on cardiac contractility in humans and rodents [72].

#### **1.4.2 Chromatin remodelling and hypertrophy**

Genomic DNA within the nuclei of eukaryotic cells is highly compacted with histone and nonhistone proteins in a dynamic polymer called chromatin. The basic unit of chromatin is the nucleosome, which comprises 146 base pairs of DNA wrapped around a histone octamer that consists of 2 copies each of histones H2A, H2B, H3, and H4. Histones control gene expression by modulating the structure of chromatin and the accessibility of regulatory DNA sequences to transcriptional activators and repressors [73]. Posttranslational modifications of histones have been proposed to establish a “code” that determines patterns of cellular gene expression [74]. Acetylation of histones by histone acetyltransferases (HAT) stimulates gene expression by relaxing chromatin structure, allowing access of transcription factors to DNA, whereas deacetylation of

histones by histone deacetylases (HDAC) promotes chromatin condensation and transcriptional repression [75].

The most extensively studied HATs in muscle are p300 and the closely related coactivator, CREB-binding protein (CBP), which play critical roles in physiological and pathological growth of cardiac myocytes [76]. The importance of p300 in normal cardiac transcription is illustrated by the phenotype of p300 knockout mice, which die between days 9 and 11.5 of gestation and show reduced expression of muscle structural proteins such as  $\beta$ -MHC and  $\alpha$ -actinin [77].

There are currently 18 known human HDACs, which fall into 3 classes based on their homology with 3 distinct yeast HDACs. Among them, class II HDACs have been shown to repress growth of myocytes [78]. In vivo, hypertrophy that is induced by activated calcineurin or pressure overload was associated with enhanced serine phosphorylation of HDAC5 and HDAC9, which suggested that chromatin-regulation could influence the hypertrophic response. HDAC5- and HDAC9-knockout mice each showed spontaneous cardiac hypertrophy with age and enhanced hypertrophy in response to pathological stimuli [79].

### **1.5 Adenoviral expression vectors**

A variety of viruses have been used for gene expression in mammalian cells, taking advantage of their ability to efficiently introduce foreign genes. Amongst the viral vectors, adenoviral vectors have been of interest because they infect a wide spectrum of mammalian cells and are capable of incorporating large DNA inserts [80]. Adenoviruses have been used to express recombinant proteins in cell lines and tissues that are otherwise difficult to transfect with high efficiency. The adenovirus vectors are capable of high efficiency in vivo gene transfer [81].

In cardiac cells it has been demonstrated that intrathoracic injection of an adenovirus encoding a reporter gene leads to infection rates of  $71 \pm 8\%$  for more than 50 days [82]. This makes adenovirus-mediated gene transfer a powerful tool to introduce desired genes in cardiomyocytes.

## 2 AIM OF THE WORK

Previous studies have demonstrated that in a transgenic model, inhibition of p53 leads to the proliferation of cardiomyocytes after myocardial infarction [32]. However, it seems difficult to separate the induction of cardiac regeneration by inactivation of the p53 gene from the increased incidence of cancer, as p53 is known to be an important tumour suppressor in mammals [49]. Manipulation of the p53-related p73 gene might offer a solution to this dilemma. Unlike p53, p73 is not a classical tumour suppressor since mutations of p73 are not typically found in malignancies and deletion of p73 does not lead to an increased tumour incidence in mice [55, 56]. Furthermore, several truncated forms of p73 are expressed under physiological conditions in various tissues such as the brain, which interfere in a dominant-negative manner with p73 and p53 [83]. Obviously, expression of truncated forms of p73 does not completely abrogate all functions of p53, since the appearance of these dominant-negative forms of p73 does not coincide with tumour formation [56].

Inspired by these findings, the aim of the presented experiments was to assess the potency of the truncated isoform p73DD to release the cell cycle arrest of cardiomyocytes thereby avoiding the potential pitfalls that are associated with a direct inactivation of the tumour-suppressor gene p53. The initial task of the study was to confirm the expression and function of adenoviral expression vectors Ad-p73DD(wt) and Ad-p73DD(mut). The second part of the work was aimed at analyzing the effects of the directed expression of p73DD in hearts of neonatal adult mice with regard to cell cycle progression and apoptosis.

### **3 MATERIALS AND METHODS**

#### **3.1 Materials**

##### **3.1.1 Mice**

$\alpha$ MHC-nlsLacZ transgenic mice were kindly provided by Dr. L. J. Field (Indianapolis, USA). In these mice, the  $\alpha$ -myosin heavy chain (MHC) promoter ensures the targeted expression of a nuclear localized  $\beta$ -galactosidase in cardiomyocytes [22]. Therefore, cardiomyocyte nuclei in mice carrying the  $\alpha$ MHC-nlsLacZ reporter transgene can be easily identified by LacZ expression (X-Gal staining or anti-LacZ immunoassay). The transgenic mice were maintained by repeated breeding with wildtype ICR mice and were identified by PCR-genotyping. All animal studies were approved by local regulatory authorities.

##### **3.1.2 Adenoviral expression constructs**

Adenoviral constructs expression N-terminal truncated mutants of human p73 were kindly provided by Dr. Henning Ebelt (Martin-Luther-University, Halle, Germany). Plasmids encoding truncated mutants of human p73 linked to an N-terminal T7-tag (p73DD) [52] were kindly provided by Dr. M. Irwin (Harvard Medical School, Boston, Massachusetts, USA). The linkage to the T7-tag fusion protein allows the expression of the p73DD proteins to be monitored using an anti-T7 immunoassay. Both the wildtype p73DD (p73DD(wt)) and a mutant p73DD which harbours a point mutation (L371P) leading to the loss of the dominant-negative properties (p73DD(mut)) were first cloned into the EcoRI-Site of pIRES2-EGFP (BD Clontech). The internal ribosomal entry site (IRES) directs translation of the enhanced green fluorescence protein, which allows the confirmation of the gene expression under fluorescence microscopy. Then the cassette containing p73DD-IRES-EGFP was excised and further cloned into pShuttle-CMV (XhoI/XbaI) of the AdEasy system for generation of recombinant adenoviruses as described [82]. Adenoviral vectors were amplified on monolayers of HEK293 cells in DMEM 2.5% FCS until complete cytopathic effect was observed, and viral titers were

determined by plaque-assay.

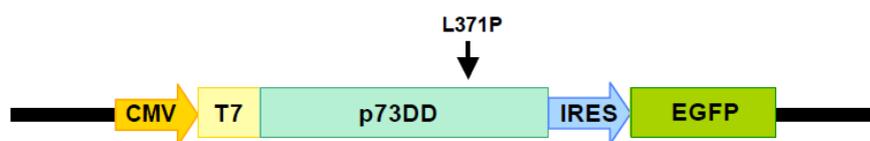


**Figure 3: A partial overview of adenoviral construct of p73DD.** N-terminal truncated mutants of human p73 linked to an N-terminal T7-tag were driven by the human cytomegalovirus (CMV) promoter, and followed by the internal ribosomal entry site (IRES), which directs translation of an enhanced green fluorescence protein (EGFP).

### 3.1.3 Chemicals

Chemical	Manufacturer
Acetic acid	Carl Roth
Aceton	Carl Roth
Agarose, for Molecular Biology	Carl Roth
Albumin, Bovine Serum (BSA)	Carl Roth
Ammonium Persulfate	Carl Roth
5-Bromo-4-chloro-3-indolyl- $\beta$ -D-galactoside	AppliChem
5-Bromo-2'-deoxyuridine	Sigma-Aldrich
Calcium Chloride	Merck
Chlorophenol red- $\beta$ -D-galactopyranoside (CPRG)	Sigma-Aldrich
Chloroform	Carl Roth
3,3'-Diaminobenzidine Tablets (DAB)	Sigma-Aldrich
Diethyl pyro-carbonate (DEPC)	AppliChem
Dimethylsulfoxid (DMSO)	Merck
Dithiothreitol (DTT)	Carl Roth
DNA Ladder (GeneRuler™ 100 bp DNA Ladder)	Fermentas
Entellan	Merck
Ethanol	Carl Roth
Ethidium Bromide	AppliChem

Ethylenediaminetetraacetic acid (EDTA)	Carl Roth
Glycerol	Carl Roth
Hemotoxyelin (Solution, Gill No.3)	Sigma-Aldrich
Hydrogen chloride	Carl Roth
Hydrogen Peroxide (30 %)	Carl Roth
Magnesium Chloride	Merck
b-Mercaptoethanol	Carl Roth
Methanol	Carl Roth
Mowiol	Calbiochem
Na-desoxycholat	Sigma-Aldrich
Nonidet P-40	Sigma-Aldrich
PageRuler™ Prestained Protein Ladder	Fermentas
Paraformaldehyde	Merck
Potassium hexacyano-ferrate (III) (K <sub>3</sub> Fe(CN) <sub>6</sub> )	Sigma-Aldrich
Potassium hexacyano-ferrate (II), trihydrate (K <sub>4</sub> Fe(CN) <sub>6</sub> 3H <sub>2</sub> O)	Sigma-Aldrich
Potassium <i>di</i> -hydrogen phosphate	Carl Roth
Sodium Chloride	Carl Roth
Sodium dodecyl sulfate (SDS)	Carl Roth
Sodium Hydroxide	Carl Roth
<i>di</i> -Sodium hydrogen phosphate	Merck
Sodium <i>di</i> -hydrogen phosphate	Merck
Sucrose	Sigma-Aldrich
POLYFREEZE™	Polysciences
2-Propanol	Carl Roth
Tetramethylethylendiamin (TEMED)	Carl Roth
Tris (base)	Carl Roth
Triton X-100	Carl Roth
VECTABOND™ Reagent	Vector Laboratories
X-Gal (5-Bromo-4-chloro-3-indolyl-b-D-galactoside)	Carl Roth
Xylene	Carl Roth

### 3.1.4 Buffers and solutions

<b>Genotyping</b>	
Proteinase K buffer	100 mM Tris-HCl, 5 mM EDTA, 0.2 % SDS, 200 mM NaCl in dH <sub>2</sub> O, pH 8.0
Tris-EDTA buffer (TE)	10 mM Tris-HCl (pH 7.5), 1 mM EDTA (pH 8.0)
<b>DNA Electrophoresis</b>	
50x TAE buffer (Tris/boric acid/EDTA buffer)	2 M Tris-acetate, 50 mM EDTA in dH <sub>2</sub> O
10 x DNA loading buffer	100 mM EDTA, 20 % Ficoll 400, 1 % SDS, 0.25 % Bromphenol blue and 0.25 % Xylencyanol, pH 7.5
<b>β-Gal assay</b>	
Z-buffer	0.06 M Na <sub>2</sub> HPO <sub>4</sub> , 0.04 M NaH <sub>2</sub> PO <sub>4</sub> , 0.01 M KCl, 1 mM β-mercaptoethanol in dH <sub>2</sub> O
CPRG buffer	50 mM CPRG stock solution 1:7 diluted in Z-buffer
<b>Immunohistological staining</b>	
10 x PBS (phosphate-buffered saline)	1.37 M NaCl, 27 mM KCl, 80 mM Na <sub>2</sub> HPO <sub>4</sub> and 18 mM KH <sub>2</sub> PO <sub>4</sub> in dH <sub>2</sub> O, pH 7.4
4% Paraformaldehyde (PFA)	4 % Paraformaldehyde in PBS, stirred and heated to 60-65 °C till the solution became clear, pH adjust to 7.2. Aliquots were stored at -20 °C
X-Gal stock solution	40 mg/ml X-Gal in DMSO, stored in dark at -20 °C
X-Gal phosphate buffer	840 ml 0.2 M Na <sub>2</sub> HPO <sub>4</sub> , 160 ml 0.2 M NaH <sub>2</sub> PO <sub>4</sub> in dH <sub>2</sub> O
X-Gal wash solution	2 ml 1 M magnesium chloride, 10 ml 1 % sodium desoxycholate, 10 ml 2 % NP-40 in X-Gal phosphate buffer
X-Gal staining solution	5 mM K <sub>3</sub> Fe(CN) <sub>6</sub> , 5 mM K <sub>4</sub> Fe(CN) <sub>6</sub> , 5 mM MgCl <sub>2</sub> , and 1 mg/ml X-Gal in PBS
Blocking solution	1 % BSA, 3 % horse serum in PBS
Permeabilization solution	0.1 % Triton X-100 in PBS
ABC solution	40 μl solution A and 40 μl solution B in 10 ml PBS, prepared 30 min before application.
DAB solution	0.67 mg/ml diaminobenzidine in 0.03% H <sub>2</sub> O <sub>2</sub> / PBS.
PBS-T	0.05 % (v/v) Tween-20 in PBS.
<b>SDS-PAGE</b>	

Ammonium persulfate stock solution	10 % (w/v) ammonium persulfate in dH <sub>2</sub> O and stored at -20 °C
4x SDS gel loading buffer	50 mM Tris, 5 % (w/v) SDS, 10% 2-mercaptoethanol and 10 % (v/v) glycerol
Tris-glycin electrophoresis buffer	23 mM Tris base, 190 mM glycine and 0.2 % SDS in dH <sub>2</sub> O, pH 8.3.
1 x Blotting buffer	14.4 g glycine, 3.03 g Tris, 200 ml methanol in dH <sub>2</sub> O, pH 8.3.
10 x TBS-T buffer	80 g NaCl, 2 g KCl, 30.3 g Tris base in dH <sub>2</sub> O, pH 7.5.
Blocking solution	5 % dried milk powder dissolved in TBS-T.
<b>RNA</b>	
DEPC (Diethylpyrocarbonat) H <sub>2</sub> O	0.1 % (v/v) DEPC in dH <sub>2</sub> O, autoclaved and aliquots.

### 3.1.5 Antibodies

#### Primary Antibodies

Anti-Bromodeoxyuridine, mouse monoclonal	Dako (M0744)
Anti-phospho-Histone H3, rabbit polyclonal	Upstate (06-570)
Anti-ACTIVE® Caspase-3, rabbit polyclonal	Promega (G7481)
Anti-AuroraB, rabbit polyclonal	Abcam (ab2254)
Anti-T7, mouse monoclonal	Novagen (69522)
Anti-p73, rabbit monoclonal	Epitomics (1636-1)
Anti-p53, mouse monoclonal	BD Science (554157)
Anti-Cyclin A, rabbit polyclonal	Santa Cruz (sc-751)
Anti-Cyclin B2, rabbit polyclonal	Santa Cruz (sc-22776)
Anti-Cyclin D1, mouse monoclonal	Cell Signaling (2926)
Anti-Cyclin D2, rabbit polyclonal	Santa Cruz (sc-593)
Anti-Cyclin D3, mouse monoclonal	Cell Signaling (2936)
Anti-Cyclin E, rabbit polyclonal	Santa Cruz (sc-481)
Anti-p15INK, rabbit polyclonal	Cell Signaling (4822)
Anti-p21WAF, mouse monoclonal	BD Science (556431)
Anti-p27, rabbit polyclonal	Cell Signaling (2552)

Anti-CDK4, mouse monoclonal	Cell Signaling (2906)
Anti-GAPDH, rabbit monoclonal	Cell Signaling (2118)

#### Secondary Antibodies

Biotinylated Anti-Mouse/Rabbit IgG (H+L), horse polyclonal	Vector Laboratories (BA-1400)
Peroxidase, Anti-Mouse IgG, horse polyclonal	Cell Signaling (7076)
Peroxidase, Anti-Rabbit IgG, goat polyclonal	Cell Signaling (7074)

### 3.1.6 Enzymes

Enzyme	Manufacturer
Neuraminidase type V	Sigma-Aldrich (N2876)
Taq polymerase, recombinant	Invitrogen (10342-020)
Proteinase K	Novagen (70663)

### 3.1.7 Kits

Kits	Manufacturer
BD™ TransFactor Extraction Kit	BD Biosciences (631921)
Pierce BCA Protein Assay Kit	Pierce (23225)
Luciferase Reporter Assay Kit	BD Biosciences (K2039-1)
SuperScript™ First-Strand Synthesis System for RT-PCR	Invitrogen (11904-018)
SuperSignal West Pico Chemiluminescent Substrate	Pierce (34079)
SuperSignal West Femto Maximum Sensitivity Substrate	Pierce (34095)
VECTASTAIN Elite ABC Kit (Standard)	Vector Laboratories (PK-6100)

### 3.1.8 Primers

Primer	Sequence	Annealing	Product
LacZ	forward:CTCTGACAGAGAAGCAGGCACTTTACATGG reverse: GCCAGGGTTTTCCCAGTCACGACGTTGT	62 °C	340 bp
ANF	forward:CGTGCCCCGACCCACGCCAGCATGGGCTCC	62 °C	494 bp

	reverse: GGCTCCGAGGGCCAGCGAGCAGAGCCCTCA		
GAPDH	forward: ACCACAGTCCATGCCATCAC	60 °C	451 bp
	reverse: TCCACCACCCTGTTGCTGTA		
p21 <sup>WAF</sup>	forward: TGTGGACATCACCCGTGACC	60 °C	793 bp
	reverse: GGAGAGGGCAGGCAGCGTAT		
cyclin A	forward: TGAGACCCTGCATTTGGCTGTGAACT	60 °C	523 bp
	reverse: CCCCAGAAGTAGCAGAGTTTGTGTA		
cyclin B1	forward: TCGATCGGTTTCATGCAGGAC	56 °C	300 bp
	reverse: AGAGCTCCATGAGGTATTTGGC		
cyclin B2	forward: AAAGCCGGAGAGGTGGATGTTG	60 °C	300 bp
	reverse: CAGGAGTCTGCTGCTGGCATAAC		
cyclin D1	forward: CCTGTGCTGCGAAGTGGAGA	60 °C	494 bp
	reverse: CTGGCATTTTGGAGAGGAAGTGT		
cyclin D2	forward: TGGCCGCAGTCACCCCTCAC	60 °C	446 bp
	reverse: TCTCTTGCCGCCCGAATGG		
cyclin D3	forward: TTCCAGTGCGTGCAAAAGGA	56 °C	592 bp
	reverse: CTCGCAGGCAGTCCACTTCA		
cyclin E	forward: TTGTGTCCTGGCTGAATGTCTATGTCC	60 °C	486 bp
	reverse: CTGCTCGCTGCTCTGCCTTCTTACT		
ANP	forward: ACCTGCTAGACCACCTGGAGGAG	65 °C	347 bp
	reverse: CCTTGGCTGTTATCTTCGGTACCGG		
BNP	forward: ATCTCCTGCAGGTGCTGTCCCAG	65 °C	369 bp
	reverse: GGTCTTCCTACAACAACCTCAGTGCGTTAC		
aMHC	forward: CTGCTGGAGAGGTTATTCCTCG	65 °C	302 bp
	reverse: GGAAGAGTGAGCGGCATCAAGG		
bMHC	forward: TGCAAAGGCTCCAGGTCTGAGGGC	65 °C	203 bp
	reverse: GCCAACACCAACCTGTCCAAGTTC		

### 3.1.9 Equipments

<b>Product</b>	<b>Manufacturer</b>
Agarose electrophoresis unit	OWI
Biofuge/pico	Heraeus Instruments (Hanau)
Biofuge/fresco	Heraeus Instruments
Cell culture incubator	Heraeus Instruments
Confocal Microscope, Leica TCS SP2	Leica
Cryostat, Leica 3050S	Leica
iCycler iQ Real-Time PCR detection system	Bio-Rad
Digital Camera COOLPIX 4500	Nikon
Fastblot B33/B34	Biometra
Fluorescence Microscope ECLIPSE/E600	Nikon
Homogenizer	IKA
Laminar flow hood	Heraeus Instruments
Light Microscope ECLIPSE/E200	Nikon
Luminometer FB12	Berthold
Microcentrifuge 5415R	Eppendorf
Micropipette	Gilson S.A.S.
PCR Thermocycler	Bio-Rad
Power-Pac 200	Bio-Rad
Shaker, Rocky 100	Labortechnik Fröbel
Mini-PROTEAN Tetra Electrophoresis System	Bio-Rad
Spectrophotometer	Bio-Rad
Vortex	IKA
Water bath DIN 40050-IP20	Memert
X-ray film processor	Kodak

## 3.2 Methods

### 3.2.1 Neonatal rat cardiomyocytes preparation

Neonatal rat cardiomyocytes from 1- to 3-day postnatal rats were isolated and cultivated as described [84]. Briefly, hearts were dissected, minced, and gently digested with dissociation solution containing 0.03 % collagenase and 0.12 % trypsin. The dissociated cells were preplated onto 175 cm<sup>2</sup> culture flasks for 1 h, allowing the quick attachment of non-cardiomyocytes. The resultant cell suspension was plated onto 25 cm<sup>2</sup> culture flasks in plating medium (DEME) supplemented with 25 µl/ml bovine serum albumin, 25 µl/ml transferrin and 25 µl/ml insulin.

### 3.2.2 Analysis of subcellular localization of p73 isoforms

HEK293 cells were plated in 150 mm plates at a density of  $5 \times 10^6$  cells per dish. They were cultured in DMEM medium with 10 % FCS and incubated in 10 % CO<sub>2</sub> at 37 °C. The next day HEK293 cells were subjected to recombinant viruses encoding p73DD(wt) or p73DD(mut) at  $10^8$  pfu/ml, respectively. Untreated cells were used as a control. After 1 h incubation with the viruses, medium was changed to DMEM with 2.5 % FCS and left for 48 h. For determination of subcellular localization of p73DD, cytoplasmic and nuclear fraction of proteins were isolated using BD<sup>TM</sup> Transfection Extraction Kit according to the manufacturer's instructions. The concentration of proteins was measured using Pierce BCA Protein Assay, and protein fractions were subjected to SDS-PAGE.

### 3.2.3 p53 reporter assay

HEK293 or H1299 (p53 knockout cell line) cells were plated in 6-well plates at a density of  $5 \times 10^5$  cells per well, respectively, and cultured in DMEM medium with 10 % FCS. The next day, cells were transfected with 4 µg of a p53-dependent luciferase plasmid containing a p53-response element (Mercury<sup>TM</sup> Profiling Vectors; Clontech) and 1 µg of a β-galactosidase plasmid using METAFECTENE<sup>TM</sup> PRO according to the manufacturer's instructions. After 24 h the cells were infected for 1 h with  $10^8$  pfu Ad-p73DD(wt), Ad-p73DD(mut), or Ad-EGFP, respectively, and subsequently cultured with DMEM with 2.5 % FCS. 24 h later, medium was aspirated and 150 µl cell lysis buffer (BD luciferase reporter assay kit) was added to each well. The lysis buffer

suspension was incubated on ice for 20 min and centrifuged at 13,000 for 1 min. The resulting supernatants were subjected to the luciferase assay according to the instruction of BD luciferase reporter assay kit. To normalize the transfection efficiency,  $\beta$ -galactosidase assay was performed. To the 10  $\mu$ l supernatants, 80  $\mu$ l CPRG buffer was added, shortly centrifuged and incubated at 37 °C. 500  $\mu$ l 1 M  $\text{Na}_2\text{CO}_3$  was immediately added to stop the reaction after the solution turned dark red, and OD 574 nm was measured using spectrophotometer.

#### **3.2.4 Isolation of genomic DNA and genotyping PCR**

For genotyping, around 0.5 cm of mouse-tail was excised. Then 500  $\mu$ l proteinase K buffer containing 200  $\mu$ g/ml proteinase K enzyme was added to the excised tails and kept for overnight digestion at 56 °C. The digested tails were vortexed briefly and centrifuged at 14,000 rpm for 10 min. The supernatant was transferred to a fresh microtube containing 500  $\mu$ l ice-cold isopropanol and mixed carefully by swirling the tubes for 3 times. Again the tubes were centrifuged at 14,000 rpm for 10 min in order to precipitate the genomic DNA. The supernatant was discarded and the DNA pellet was washed with 70 % ethanol by centrifuging at 14,000 rpm for 10 min at RT. Ethanol was then discarded and tubes were air dried to get rid of excess ethanol. The DNA pellet was dissolved in 100  $\mu$ l TE buffer (pH 7.5) and stored at -20 °C.

PCR was used for genotyping following DNA isolation. Amplification of the ANF gene, which generally exists in mouse genomic DNA, serves as an internal control to assess the quality of DNA preparation. LacZ gene fragment was only detectable in the transgenic mice by using LacZ primers. PCR reaction was prepared in 25  $\mu$ l total volume containing 1  $\mu$ l genomic DNA template, 0.3 U Taq-polymerase, 5 nmol forward primer and reverse primer respectively, 10  $\mu$ mol dNTPs, 1.5 mM  $\text{MgCl}_2$  and 2.5  $\mu$ l Taq-polymerase buffer. The PCR program was performed with activating the enzyme and denaturing the DNA template at 95 °C for 5 min, followed by 40 cycles of DNA denaturation at 95 °C for 1 min, annealing at 62 °C for 2 min and extension at 72 °C for 3 min, and the final extension at 72 °C for 10 min. The PCR products were analyzed on a 1.5 % agarose gel marked with 100 bp DNA marker (Fig. 4).

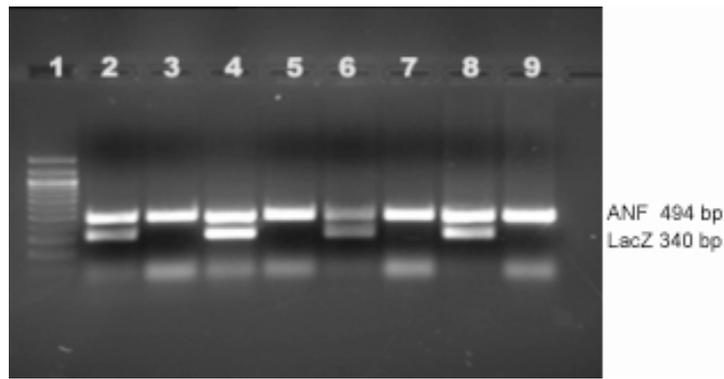


**Figure 4: LacZ genotyping PCR.**

Lane 1: 100bp DNA marker.

Lane 2-7: DNA samples from mice, in which Lane2, 4 and 6 indicated transgenic mouse.

Lane 8: aMHC-nLacZ positive control.

Lane 9: aMHC-nLacZ negative control.

### 3.2.5 Intrathoracic injection

The progeny of LacZ and ICR mice were designated into three groups: Ad-p73DD(wt), Ad-p73DD(mut) and control group, respectively. For the adenovirus-treated groups, on the day of birth the neonatal mice were anesthetized by cooling on ice for approximately 2 min and put in front of cold light source to visualize the silhouette of the heart. Using a Hamilton syringe, a total volume of 10  $\mu$ l recombinant virus ( $10^8$  pfu) was injected into the thoracic cavity beside the heart at a left parasternal position. Finally the animals were re-warmed and put back to their mothers. The mice who served as control group were untouched on the day of birth. On the 7<sup>th</sup> day after birth, all the mice were numbered by ear marking and tails were excised for PCR genotyping. On the 13<sup>th</sup> day after birth, the LacZ-transgenic mice were injected with BrdU (100 mg/kg body weight) and on the following day all the animals (both LacZ-transgenic and non-transgenic mice) were sacrificed by cervical dislocation. Lungs, livers and hearts were isolated, washed with PBS, and the individual organ weights were then determined. The hearts were checked under fluorescence microscope for EGFP expression to give a brief estimate of viral transfection efficiency. The LacZ-positive hearts (detected by genotyping as described above) were preserved for histological analysis. Briefly, the hearts were incubated in 30 % sucrose overnight at 4 °C and then freezeed in POLYFREEZE<sup>TM</sup> using dry ice. The tissue sections were prepared at 10  $\mu$ m

thickness and dried for 30 minutes before placing back to -20 °C freezer where they were kept until use.

The LacZ-negative hearts were immediately dipped in liquid nitrogen and used for mRNA- and protein-expression analysis.

### **3.2.6 Intramyocardial injection**

Adult  $\alpha$ MHC-nlsLacZ transgenic mice were used in this part of the study. On day 0, mice were initially anesthetized with inhalational isoflurane (95 % oxygen and 5 % isoflurane) and ventilated at 200 breaths/min through a plastic tube placed in the trachea using a rodent ventilator. Anesthesia was maintained subsequently with 2.5 % isoflurane delivered in O<sub>2</sub> through the ventilator. Ketotifen (5 mg/kg) was administered preoperatively for analgesia and the operation was performed on a heated table (38 °C) to maintain body temperature. An incision was made into the skin to the left of the sternum and the underlying muscle layers were dissected. After thoracotomy in the fourth intercostal space, hearts were exposed and adenoviral vector was directly injected into the myocardium of the left ventricle. The ribs, muscle and skin layers were then closed separately. The mice were allowed to recover and transferred to the cage. On day 3 and 4, they received two times an injection of BrdU (100 mg/kg BW) intraperitoneally and were finally sacrificed on day5 by cervical dislocation. Liver, lung and heart were isolated, washed and weighed separately. The hearts were put into 30 % sucrose/PBS at 4 °C overnight, then placed in POLYFREEZE™ and put on the dry ice until the tissue matrix had frozen completely. The tissue block was place on the cryostat specimen disk and 10  $\mu$ m frozen sections were prepared followed by drying for 30 min at RT. The slides were kept at -20 °C until staining.

### **3.2.7 Immunohistochemical staining**

#### **LacZ staining**

Before performing immunostaining, tissue slides were stained with X-gal in order to identify the cardiomyocyte nuclei (blue signal; derived from  $\alpha$ MHC-nlsLacZ transgene). Briefly, slides were washed three times with PBS solution for 10 min each, then once with X-gal wash solution for 10 min. The slides were then immersed in X-gal staining solution and incubated at 37 °C. Once the cardiomyocytes' nuclei turned blue, the slides were washed with PBS solution and preceded with immunostaining.

**BrdU immunoassay**

At this step, slides were first fixed with 70% methanol/ 30% acetone at RT for 15 min. They were then immersed in 3% H<sub>2</sub>O<sub>2</sub>/ methanol solution to block endogenous peroxidase activity and then treated with permeabilization solution for 15 min. For BrdU immunoassay, slides were incubated with 4 N HCl to denature the double-stranded genomic DNA. Before applying the primary antibody, unspecific binding sites were first blocked using immunohistological blocking solution at RT for 30 min and afterwards slides were incubated with BrdU antibody (1:1000 in 1 % BSA) at RT for 2 h. After washing with PBS and 1 % BSA/PBS, they were incubated with a biotinylated anti-mouse/rabbit IgG antibody (1:1000 in PBS) at RT for 1 h. The immunoactive signal was amplified by incubating slides with ABC solution (VECTASTAIN Elite ABC Kit) for 30 min, and visualized using DAB solution. Finally, the slides were dehydrated with series of alcohols (70 % ethanol – 96 % ethanol – Xylol) and covered with coverslips using entellan.

**T7 immunoassay**

Slides were first fixed with 70% methanol/ 30% acetone at RT for 15 min. They were then immersed in 3% H<sub>2</sub>O<sub>2</sub>/ methanol solution to block the endogenous peroxidase activity and then treated with permeabilization solution for 15 min. Before applying the primary antibody, unspecific binding sites were first blocked using immunohistological blocking solution at RT for 30 min and slides were incubated with a T7-antibody (1:100 in 1 % BSA) at 4 °C overnight. After washing with PBS and 1 % BSA/PBS, they were incubated with a biotinylated anti-mouse/rabbit IgG antibody (1:1000 in PBS) at RT for 1 h. The immunoactive signal was amplified by incubating slides with ABC solution (VECTASTAIN Elite ABC Kit) for 30 min, and visualized using DAB solution. Finally, slides were dehydrated with series of alcohols (70 % ethanol – 96 % ethanol – Xylol) and covered with coverslips using entellan.

**Phosphorylated histon3 immunoassay**

Slides were first fixed with 70% methanol/ 30% acetone at RT for 15 min. They were then immersed in 3% H<sub>2</sub>O<sub>2</sub>/ methanol solution to block the endogenous peroxidase activity and then treated with permeabilization solution for 15 min. Unspecific binding sites were first blocked using immunohistological blocking solution at RT for 30 min and slides were incubated with phospho-H3 antibody (1:1000 in 1 % BSA) at RT for 2

h. After washing with PBS and 1 % BSA/PBS, they were incubated with biotinylated anti-mouse/rabbit IgG antibody (1:1000 in PBS) at RT for 1 h. The immunoactive signal was amplified by incubating slides with ABC solution (VECTASTAIN Elite ABC Kit) for 30 min, and visualized using DAB solution. Finally, slides were dehydrated with series of alcohols (70 % ethanol – 96 % ethanol – Xylol) and covered with coverslips using entellan.

#### **AuroraB immunoassay**

Slides were first fixed with 10 % neutral buffered formalin at RT for 15 min. They were then immersed in 3% H<sub>2</sub>O<sub>2</sub>/ methanol solution to block the endogenous peroxidase activity and then treated with permeabilization solution for 15 min. Unspecific binding sites were first blocked using immunohistological blocking solution at RT for 30 min and slides were incubated with AuroraB antibody (1:300 in 1 % BSA) at 4 °C overnight. After washing with PBS and 1 % BSA/PBS, they were incubated with biotinylated anti-mouse/rabbit IgG antibody (1:1000 in PBS) at RT for 1 h. The immunoactive signal was amplified by incubating slides with ABC solution (VECTASTAIN Elite ABC Kit) for 30 min, and visualized using DAB solution. Finally, slides were dehydrated with series of alcohols (70 % ethanol – 96 % ethanol – Xylol) and covered with coverslips using entellan.

#### **Activated caspase3 immunoassay**

Slides were first fixed with 4 % PFA at RT for 15 min. They were then immersed in 3% H<sub>2</sub>O<sub>2</sub>/ methanol solution to block the endogenous peroxidase activity and then treated with permeabilization solution for 15 min. Before applying primary antibody, unspecific binding sites were first blocked using immunohistological blocking solution at RT for 30 min and slides were incubated with activated caspase3 antibody (1:100 in 1 % BSA) at 4 °C overnight. After washing with PBS and 1 % BSA/PBS, they were incubated with biotinylated anti-mouse/rabbit IgG antibody (1:1000 in PBS) at RT for 1 h. The immunoactive signal was amplified by incubating slides with ABC solution (VECTASTAIN Elite ABC Kit) for 30 min, and visualized using DAB solution. Slides were counterstained with hematoxylin solution at RT for 5 min. Finally, slides were dehydrated with series of alcohols (70 % ethanol – 96 % ethanol – Xylol) and covered with coverslips using entellan.

### **3.2.8 Myocyte cross-sectional area (MCSA) and interstitial collagen fraction (ICF) determination**

Slides were fixed with 4 % PFA at RT for 15 min. After treating with 3.3 U/ml neuroaminidase type V at 37 °C for 1 h, slides were incubated with fluorescein-conjugated peanut agglutinin at 37 °C for 2 h to stain the extracellular collagen thereby delineating myocyte cross-sectional area (MCSA). Adjacent slides were fixed with 4 % PFA for 15 min and incubated with rhodamine-labeled griffonia simplicifolia lectin I (GSL-I) at RT for 2 h to selectively stain the capillaries.

Slides were then photographed using a laser scan microscope, and the cross-sectional area of individual myocytes was measured by image analyze software (Image J, NIH). Additionally, the total surface area (microscopic field), the interstitial space (total collagen) and area occupied by capillaries alone were measured by image analyze software (Image J, NIH). Interstitial collagen fraction was calculated by percent total surface area occupied by the interstitial space minus the percent total surface area occupied by the capillaries [85].

### **3.2.9 Analysis of mRNA expression**

#### **Isolation of mRNA**

Commercial available Trizol reagent was used to isolate total RNA according to manufacturer's instructions. First, the pestle of the homogenizer was dipped in 1 M NaOH for 10-15 min, then in DEPC water and was again washed with RNase digesting spray. The heart samples were taken out of the -80 °C freezer, shortly immersed in liquid nitrogen and kept on ice. Per heart, 1 ml of Trizol reagent was added and the sample was homogenized. To the homogenate, 200 µl chloroform were added and kept at RT for 10 min, then centrifuged at 12,000 g for 15 min at 4°C. The immiscible clear supernatant was taken to a fresh tube and 500 µl isopropanol were added and kept at RT for 15 min, then centrifuged at 12,000 g for at 4 °C for 15 min. The supernatant was discarded and the pellet was washed twice with 1 ml 75% ethanol. The pellet was air dried to get rid of excess ethanol. The dried pellet was then dissolved in 25 µl DEPC water and kept at 60 °C for 10 min. The concentration of RNA was determined by measuring OD at 260/280 nm. Additionally, RNA quality was assessed by gel electrophoresis.

### **Microarray analysis**

Mouse hearts from 7 days after virus injection were homogenized in Trizol reagent and then shipped to Max Planck Institute of Heart and Lung Research (Prof. Dr. Dr. Thomas Braun, Bad Neuheim, Germany). Microarray analysis was performed using Affymetrix Mouse Genome 430 2.0 Microarray, and the results of the gene expression quantifications were sent back for further analysis.

### **Reverse transcription and quantitative Real-Time PCR**

To analyze mRNA expression by PCR, the RNA samples were first converted into a single-stranded cDNA template using SuperScript<sup>TM</sup> First-Strand Synthesis System for RT-PCR. For that, 10 µg mRNA were added to 2 µl Oligo dT-primer and the final volume was made up to 21 µl with water. Then the samples were shortly centrifuged and incubated at 65 °C for 10 min. Reverse transcription reaction mixture (8 µl 5 x Transcription buffer, 4 µl DTT, 4 µl 10 mM dNTPs, 1 µl RNasin and 1 µl reverse transcriptase) was added and incubated at 42 °C for 90 min. After incubation the volume of the reaction mix was made to 400 µl with normal water and stored at -20 °C. PCR reaction was prepared in 25 µl total volume containing 10 µl cDNA template, 0.3 U Taq-polymerase, 5 nmol forward and reverse primer, 10 µmol dNTPs, 1.5 mM MgCl<sub>2</sub>, 2.5 µl Taq-polymerase buffer, 10 µmol dNTPs, 0.25 µl 100 times fluorescein, and 0.5 µl 10 times SybrGreen I. Real-Time PCR was performed with activating the enzyme and denaturing the DNA template at 95 °C for 8 min, followed by 45 cycles of DNA denaturation at 95 °C for 1 min, annealing at the desired temperatures (see table 3.1.8) for 30 s and extension at 72 °C for 1 min. Melting curve analysis was performed to ensure amplification of the intended fragments.

Relative expression level of a gene of interest (geneX) is shown as follows: expression level = [(copy number geneX per µl cDNA) / (copy number GAPDH per µl cDNA) x 1000].

#### **3.2.10 Analysis of protein expression**

##### **Protein isolation**

Heart samples were taken from -80 °C freezer and put on the ice. 30 mg tissue samples were homogenized in 400µl RIPA-buffer (50 mM Tris-HCl, pH 7.4, 1 % Triton X-100, 0.2 % sodium deoxycholate, 0.2 % SDS, 1 mM EDTA) containing 1 mM

phenylmethylsulfonyl fluoride (PMSF), 5 µg/ml aprotinin and 5 µg/ml leupeptin. The homogenates were centrifuged at 4 °C for 30 min and the supernatant were taken to a fresh microtube. Protein concentration was determined using Pierce BCA Protein Assay Kit and subjected to SDS-PAGE.

### **SDS-PAGE (Sodium dodecylsulfate polyacrylamide gel electrophoresis)**

Appropriate percentage of SDS-PAGE gel was prepared according the molecular weight of the protein of interest. 30 µg protein samples were mixed with loading buffer, heated at 95 °C for 5 min and then quickly spun down. Protein lysates were loaded and separated by running the gel at a constant current of 20 mA per gel until the bromophenol blue marker reached the bottom of the gel. After electrophoresis the gel was placed in blotting buffer. Nitrocellulose membrane, filter paper and sponge pads were soaked in the blotting buffer and nitrocellulose membrane was placed to the positive side of the gel. Blotting was carried out at 360 mA for 1 h. After blotting, the membrane was washed in TBT buffer for 5 minutes. Nonspecific protein binding sites were blocked using the blocking solution for 1 h at RT. The membrane was incubated with primary antibodies overnight at 4 °C. Immunoreactive proteins were visualized with corresponding HRP-conjugated secondary antibodies on Bio-light films using the SuperSignal West Pico or West Femto detection solutions. Blots were scanned and analyzed using ImageJ.

### **Immunoprecipitation**

Cultured neonatal rat cardiomyocytes were infected with recombinant adenoviruses at  $10^8$  pfu/ml. After 48 h, the cells were harvested with ice-cold cell lysis buffer (RIPA) and protein concentration was determined by BCA assay. 100 µg cell lysates were incubated with 30 µl Dynabeads® Protein A (Invitrogen) for 30 min at 4 °C to eliminate molecules that unspecifically bind to Protein A. Followed by magnetic separation, the supernatants were transferred to new tubes and incubated with p73 antibody (1:50 in PBS) with gentle rocking overnight at 4 °C to form an antibody-antigen complex. On the next day, 30 µl Dynabeads® Protein A were added into the cell lysates and incubated at 4 °C for 1 h to capture the antibody-antigen complex. The immunocomplexes were eluted from the Dynabeads® Protein A by heating for 5 min at 95 °C using SDS sampling buffer, and then subjected to SDS-PAGE.

### **3.2.11 Statistical analysis**

All data are presented as means  $\pm$  standard error of the mean (SEM). Statistical significance was analyzed by either t-test or analysis of variance (ANOVA).  $p < 0.05$  was considered statistically significant.

## 4 RESULTS

### 4.1 Subcellular localization of p73DD(wt) and p73DD(mut)

In order to determine the subcellular localization of the recombinant p73DD proteins, HEK293 cells were infected with adenoviruses which encode p73DD(wt) and p73DD(mut), respectively. Noninfected cells were used as control. After 48 h, the protein lysates from individually treated cells were separated into nuclear and cytoplasmic fractions and subjected to SDS-PAGE. The resulting nitrocellulose membrane was analyzed using a T7-tag antibody, which ensured the detection of recombinant p73DD proteins, but not the endogenous p73 proteins.

As shown in Fig. 5, the T7-tag antibody detected proteins of 35 kDa, which corresponds to the expected molecular weight of the p73DD proteins. Additionally, p73DD was not found in the cytoplasmic, but exclusively in the nuclear fraction.

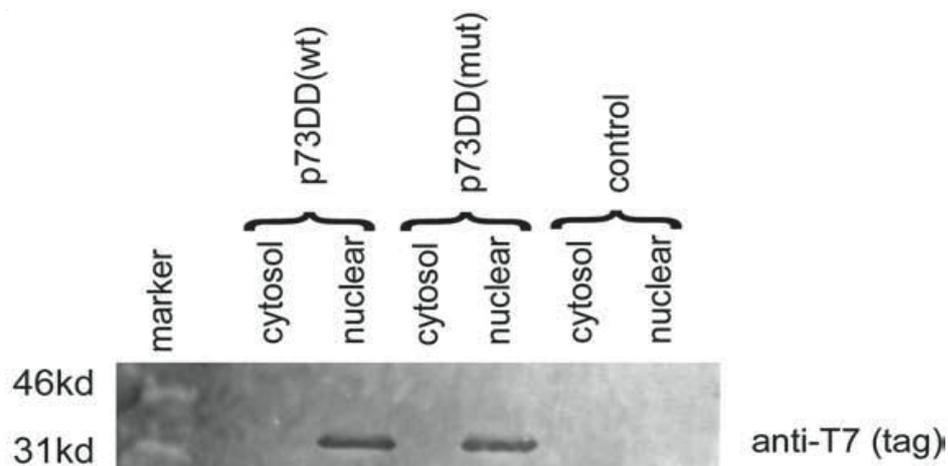


**Figure 5: Subcellular localization of p73DD proteins in HEK293 cell line (kindly provided by P. Gajawada, Universitätsklinik und Poliklinik für Innere Medizin III, Halle (Saale)) [86].** HEK293 cells were infected with recombinant adenoviruses encoding p73DD(wt) and p73DD(mut). Protein lysates were harvested and separated to cytoplasmic and nuclear fraction after 48 hours, and subjected to SDS-PAGE. Recombinant p73DD proteins (35 kDa), detected using an anti-T7 antibody, are exclusively found in the nuclear fraction.

## 4.2 p53 luciferase reporter assay

To investigate the interference of p73DD proteins on p53/p73-dependent transcription, a p53-dependent luciferase reporter assay was applied. This assay relies on the inhibition of a luciferase reporter gene expression driven by a p53-responsive promoter. To exclude any unspecific effects of the viral constructs, an adenovirus encoding EGFP (Ad-EGFP) was used as an internal viral control. Expression of p73DD(wt) significantly reduced the level of the luciferase reporter gene expression in comparison to Ad-EGFP group (Fig. 6). As expected, p73DD(mut), which carries a point mutation and thereby lacks its dominant-negative property, only had minor effects on the reporter gene expression.

To further elucidate the biological properties of p73DD(wt), H1299 cells (p53 knockout cell line) was additionally used. Similar results were observed in H1299 cells, in which induction of the luciferase reporter gene exclusively depends on the activity of endogenous p73 (Fig. 6).

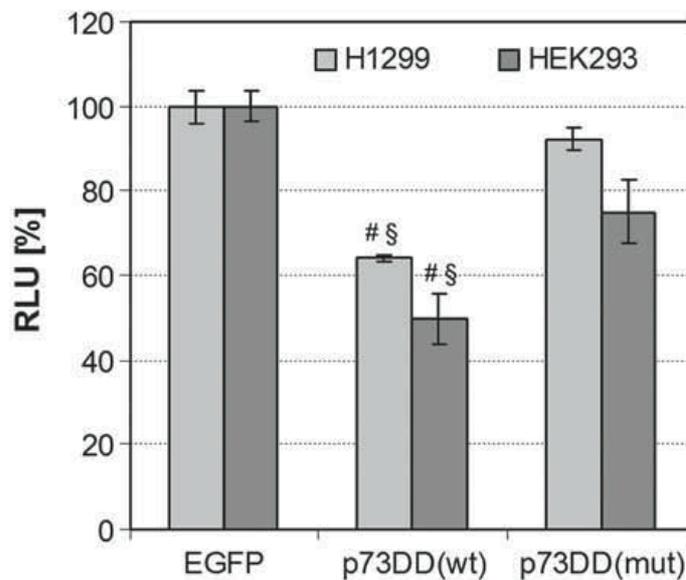


**Figure 6: p53 luciferase reporter assay [86].** Cultured cells were first transfected with a p53-dependent luciferase plasmid (and a galactosidase plasmid to control for transfection efficiency). After 24 hours, cells were then infected with Ad-p73DD(wt), Ad-p73DD(mut), or Ad-EGFP, respectively. p73DD(wt) significantly reduces p53-/p73-dependent transcription of the luciferase reporter gene as seen from reduced light emission both in HEK293 and in H1299 (p53<sup>-/-</sup>) cells. <sup>#</sup>P < 0.05 vs Ad-EGFP; <sup>§</sup>P < 0.05 vs Ad-p73DD(mut).

### 4.3 Regulation of endogenous p53 and p73 after expression of p73DD(wt)

In order to determine the effects of the recombinant p73DD proteins on the regulation of endogenous p53 and p73, neonatal rat cardiomyocytes were infected with recombinant adenoviruses encoding p73DD(wt), p73DD(mut), respectively. After 48 h, protein lysates were harvested and subjected to SDS-PAGE.

As seen from the examples given in Fig. 7, expression of p73DD(wt) led to the induction of p53 protein expression (feed-back regulation).

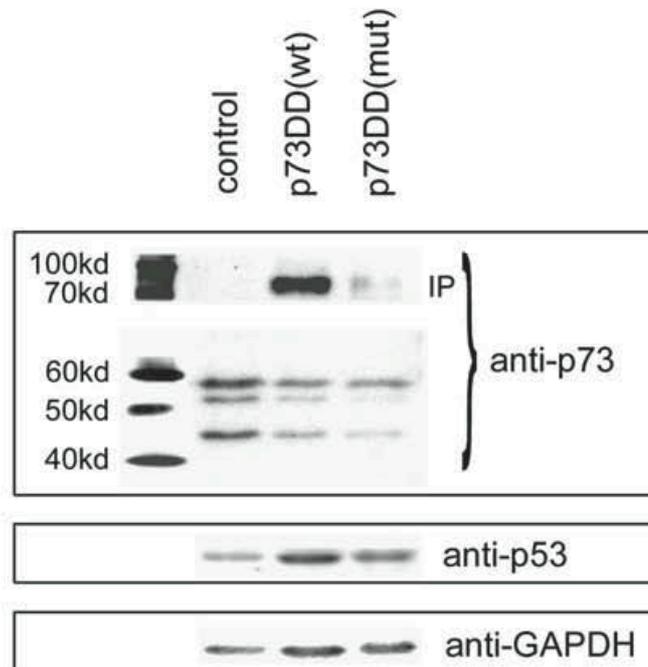


**Figure 7: Western blot analysis of p53 and p73 protein level after expression of p73DD proteins in neonatal rat cardiomyocytes [86].** Cells were infected with indicated recombinant adenoviruses and protein lysates were harvested after 48 h and subjected to SDS-PAGE. p73DD(wt) induced expression of full-length p73 as well as p53 protein. IP: immunoprecipitation.

However, full-length p73 proteins were not detectable in lysates from neonatal rat cardiomyocytes by western blot using an antibody which doesn't react with the truncated p73DD-isoforms, whereas several endogenous p73 protein isoforms with low molecular weight were detected (Fig. 7). Expression of these p73 derivatives was suppressed both by p73DD(wt) and p73DD(mut). Interestingly, immunoprecipitation analysis revealed an induction of full-length p73 protein (feed-back regulation) in

lysates treated with p73DD(wt) whereas only a minor up-regulation of p73 was seen in p73DD(mut)-infected neonatal rat cardiomyocytes (Fig. 7).

#### 4.4 Microarray analysis of gene expression after directed expression of p73DD(wt) in neonatal mouse hearts

Since activation of p53 is known to be a crucial event during the cell cycle exit of cardiomyocytes in the perinatal period, the effects of directed expression of p73DD on cardiomyocyte gene expression were first analyzed.

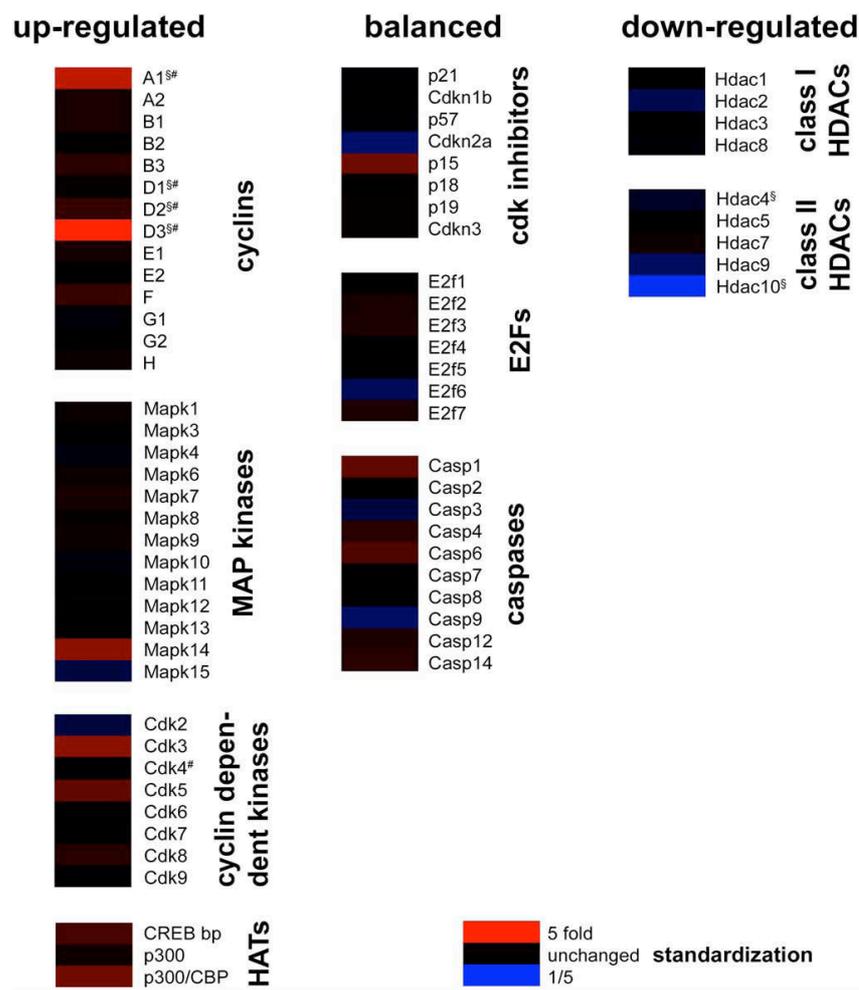


**Figure 8: Microarray analysis of gene expression in neonatal mice hearts 7 days after intrathoracic injection of p73DD(wt) in comparison to p73DD(mut) [86].** (n=3; Affymetrix Mouse Genome 430 2.0 Microarray, kindly performed by Prof. Dr. Dr. Thomas Braun, Max Planck Institute of Heart and Lung Research, Bad Neuheim, Germany). <sup>§</sup> confirmed by real-time PCR; <sup>#</sup> confirmed by Western blot.

p73DD (wildtype and mutant, respectively) was expressed in the neonatal mice hearts using adenoviral vectors as described. At day 7, neonatal hearts were removed and their mRNA expression was analyzed by microarray hybridization (Fig. 8). Directed expression of p73DD(wt) resulted in an induction of the mRNA expression of key cell cycle regulators, such as A- and D-type cyclins as well as several cyclin dependent kinases. Additionally, p73DD(wt) expression had a severe impact on the expression of histone modifying enzymes. Both class I and II histone deacetylases were suppressed whereas histone acyltransferases were upregulated. Unexpectedly, however, the expression of E2F transcription factors was not changed after p73DD expression.

#### 4.5 Effects of directed expression of p73DD(wt) on neonatal mouse hearts

##### 4.5.1 Expression of p73DD proteins in neonatal mouse hearts

Since p73DD(wt) leads to a change of the expression of several cell cycle regulating genes as seen from the microarray analysis, experiments were designed to investigate whether the activation of these genes would indeed translate into cardiomyocyte proliferation. Again, the p73DD proteins were expressed in the neonatal hearts using adenoviral vectors. 3 days after injection, a robust expression of p73DD(wt) and p73DD(mut) was detected on the histological sections using the T7-tag antibody (Fig. 9).

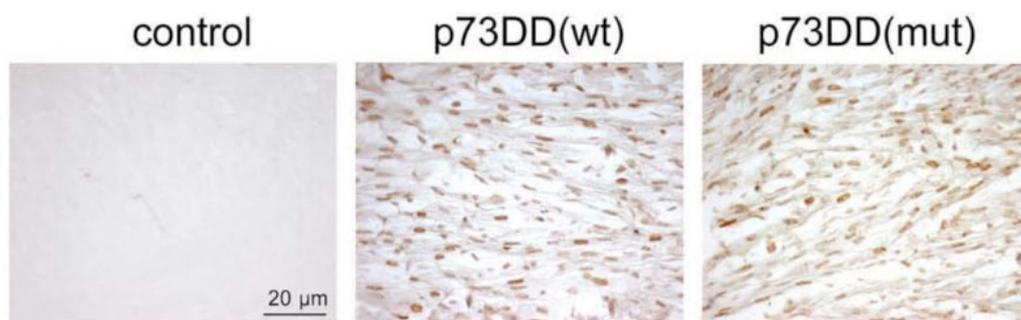


**Figure 9: Expression of p73DD 3 days after intrathoracic injection [86].** Immunostaining using a T7-tag antibody was performed on histological sections. T7-positive cells were exclusively detected in the adenovirus-injected hearts (brown signal, horseradish peroxidase-conjugated secondary antibody).

#### 4.5.2 Effects on cardiomyocyte cell cycle activity

Morphometric analysis of the neonatal hearts after 3 days revealed a significantly increased relative heart weight in the p73DD(wt)-injected hearts (Tab. 1). To explore whether the increased relative heart weight resulted from the induction of cardiomyocyte proliferation, histological analysis of cardiomyocyte cell cycle activity was performed.

BrdU is a thymidine analog, which is able to incorporate into DNA double-strand during S-phase of the cell cycle. Thus, DNA-synthesizing cells can be detected on histological sections by anti-BrdU immunoassay. In control hearts, only 0.67 % of all cardiomyocytes (identified by LacZ-staining; see method section 3.2.7) were BrdU-positive. A similar level of BrdU-positive cardiomyocytes was found in the p73DD(mut)-injected hearts. In contrast, p73DD(wt)-injected hearts revealed a significantly higher rate of cardiomyocytes who underwent DNA-synthesis in comparison to both the control and p73DD(mut)-injected hearts (Tab. 1).

DNA synthesis alone, however, does not indicate that cells finally complete the cell cycle and divide. It remains possible that cardiomyocytes are arrested in G2/M-phase. Therefore, sections from the different groups were screened for the presence of Aurora B activity, which is a marker of cytokinesis. In the control hearts of 3 days old animals, totally 14,218 cardiomyocytes were counted, however, none of them was under cytokinesis at basal conditions. Again, a comparable low level of cardiomyocyte Aurora B activity was detected after directed expression of p73DD(mut), whereas expression of p73DD(wt) led to a significant rise of the number of Aurora B-positive cardiomyocytes (Tab. 1; Fig. 10: J-L).

**Table 1:** Relative heart weights, cardiomyocyte cross sectional area (MCSA) and parameters of cell cycle activity 3 days after expression of the indicated adenoviruses in neonatal mice [86]

Parameter	Control (n=13)	p73DD(wt) (n=9)	p73DD(mut) (n=13)
Relative heart weight [mg/g]	6.9 ± 0.2	7.7 ± 0.3 <sup>§</sup>	7.2 ± 0.2
BrdU-positive CM	42/6275 (=0.67%)	108/9450 (=1.9%) <sup>§,#</sup>	78/8224 (=0.95%)
AuroraB-positive CM	0/14,218 (=0%)	6/14,607 (=0.04%) <sup>§</sup>	0/14,868 (=0%)
MCSA [ $\mu\text{m}^2$ ]	12.8 ± 0.4	10.4 ± 0.6 <sup>§</sup>	11.2 ± 0.3

<sup>§</sup>p<0.05 vs. control; <sup>#</sup>p<0.05 vs. p73DD(mut)

To test whether p73DD(wt) expression leads to sustained proliferation of cardiomyocytes, hearts at later developmental stages were analyzed. Expression of p73DD(wt) led to a moderate but significant increase of the relative heart weight 14 days after the virus injection in comparison to untreated hearts, whereas the relative weights of liver and lung did not change (Tab. 2). No significant change of relative heart weight was noted after expression of p73DD(mut). Signs of cardiomyocyte proliferation were also observed in the p73DD(wt) hearts as indicated by a significantly increased number of both BrdU-positive (Tab 2; Fig. 10: A-C) and phosphorylated histone3-positive (a marker for mitosis) cardiomyocytes (Tab. 2; Fig. 10: G-I).

**Table 2:** Relative heart, lung, liver weights, parameters of cell cycle activity, apoptosis and myocyte cross-sectional area (MCSA) 14 days after expression of the indicated adenoviruses in neonatal mice (kindly provided by P. Gajawada, Universitätsklinik und Poliklinik für Innere Medizin III, Halle (Saale)) [86].

Parameter	Control (n=15)	p73DD(wt) (n=26)	p73DD(mut) (n=11)
Relative heart weight [mg/g BW]	6.1 ± 0.2	6.8 ± 0.2 <sup>§</sup>	6.5 ± 0.2
Relative lung weight [mg/g BW]	13.4 ± 0.2	13.1 ± 0.3	13.6 ± 0.3
Relative liver weight [mg/g BW]	37.0 ± 0.8	36.7 ± 0.5	40.5 ± 0.7
BrdU-positive CM	1/120,182 (=0.001%)	17/191,109 (=0.009%) <sup>§,#</sup>	3/141,922 (=0.002%)
PhosphoH3-positive CM	0/109,030 (=0%)	10/166,718 (=0.006%) <sup>§</sup>	2/124,326 (=0.002%)
Activated caspase3-positive cells	23/153,790	23/168,726	28/162,236
MCSA [ $\mu\text{m}^2$ ]	73.1 ± 3.2	88.9 ± 0.8 <sup>§,#</sup>	72.1 ± 1.6

<sup>§</sup>p<0.05 vs. control; <sup>#</sup>p<0.05 vs. p73DD(mut).

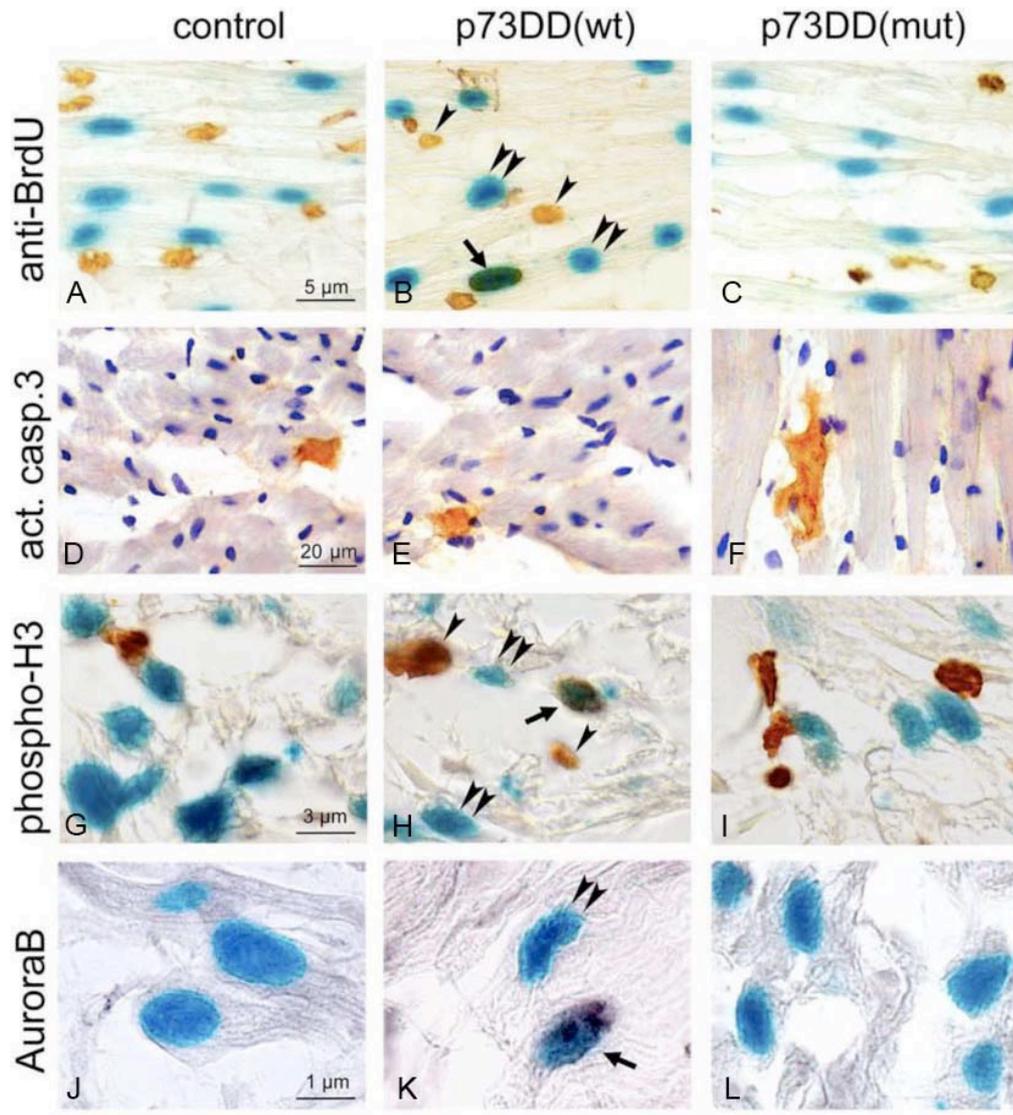


**Figure 10: Examples of photographs taken from mouse heart histological sections after directed expression of the indicated adenoviruses [86]. (A-C) BrdU staining. Cardiomyocyte nuclei (transgenic mouse aMHC-nlsLacZ) were first visualized by X-Gal staining, and DNA-synthesizing cells were identified by anti-BrdU immunoassay. Arrow: BrdU-positive cardiomyocyte; Single arrowhead: BrdU-positive non-cardiomyocyte; Double arrowhead: BrdU-negative cardiomyocyte. (D-F) Apoptosis assay detected with activated caspase 3 immune reactivity. Nuclei were counterstained with hematoxyline. (G-I) Phosphorylated histon H3 staining. Cardiomyocyte nuclei were visualized by X-gal staining. Arrow: pH3-positive cardiomyocyte; single arrowhead: pH3-positive non-cardiomyocyte; double arrowhead: pH3-negative cardiomyocytes. (J-L) AuroraB staining. Cardiomyocyte nuclei were visualized by X-gal staining. Arrow: AuroraB-positive cardiomyocyte; double arrowhead: AuroraB-negative cardiomyocyte. Images (J-L) were taken from 3-day-old mice, others were taken from 14-day-old mice.**

### 4.5.3 Effects on cell growth of cardiomyocytes

To determine whether cardiac hypertrophy also contributed to the increased relative heart weight of the mice treated with Ad-p73DD(wt), myocyte cross-sectional area (MCSA) was determined on the histological sections. It is of interest to note that at early developmental stages, p73DD(wt) expression led to a significant reduction in the size of cardiomyocytes in comparison to the control hearts (Tab. 1). However, this situation was obviously changed 14 days after the virus injection, as seen in Tab. 2, the mean size of the cardiomyocytes in p73DD(wt) group was significantly larger than seen in control and p73DD(mut) groups (Fig. 11A).

Further analysis of cardiac hypertrophic cell growth 14 days after p73DD(wt) expression revealed that the increase of cardiomyocyte size was accompanied by an increase of the expression of BNP, the  $\beta$ -MHC-isoform (Tab. 3) as well as a significant increase of interstitial fibrosis (Fig. 11B), which are hallmarks of “pathological” hypertrophy. Meanwhile, increased expression level of PKB and  $\beta$ -catenin, which are generally believed to represent markers of “physiological” cell growth, was also detected in p73(wt)-injected hearts by Western blot analysis.

**Table 3:** mRNA expression 14 days after expression of the indicated adenoviruses in neonatal mice (n = 4 per group) [86].

Gene	control	p73DD(wt)	p73DD(mut)
ANP [deltaCT GAPDH]	1.41 $\pm$ 0.70	1.65 $\pm$ 0.14	1.13 $\pm$ 0.62
BNP [deltaCT GAPDH]	0.12 $\pm$ 0.04	0.23 $\pm$ 0.04	0.18 $\pm$ 0.05
bMHC/aMHC [x 10 <sup>3</sup> ]	1.61 $\pm$ 0.18	2.71 $\pm$ 0.40 <sup>§</sup>	2.29 $\pm$ 0.34

<sup>§</sup>p<0.05 vs. control

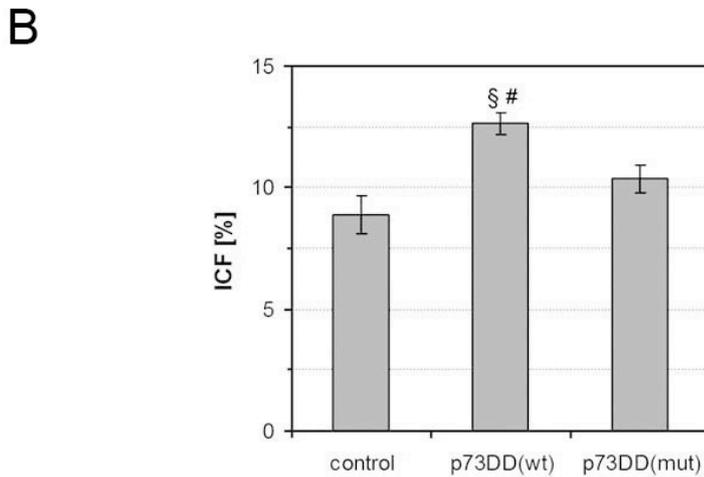
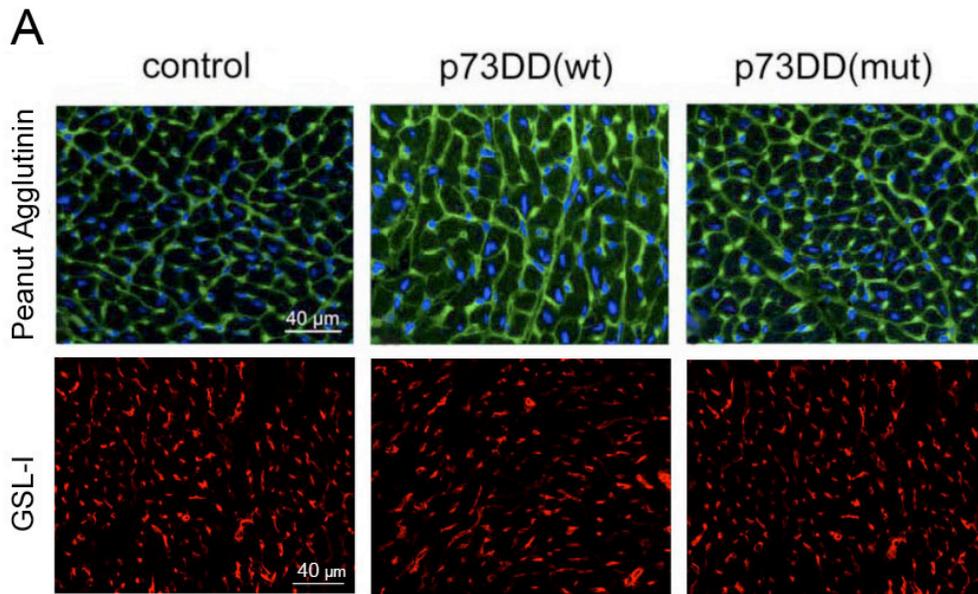


**Figure 11: Analysis of myocyte cross-sectional area (MCSA) and interstitial collagen fraction (ICF) in hearts at day 14 after injection of recombinant adenovirus (n=5 per group) [86].** A, Interstitial collagen staining with peanut agglutinin delineates the myocyte cross-sectional area. GSL-I staining selectively binds to interstitial capillaries. B, Interstitial collagen fraction was calculated by percent total surface area occupied by the interstitial space (green pixel) minus the percent total surface area occupied by the capillaries (red pixel). <sup>§</sup>p<0.05 vs. control; <sup>#</sup>p<0.05 vs. p73DD(mut).

#### 4.5.4 Effects on cardiomyocyte apoptosis

It is well known that activation of oncogenes, which activates the cardiomyocyte cell cycle progression, often results in induction of apoptosis. Here, the effect of directed

expression of recombinant adenoviruses on this type of cell death was examined by staining activated caspase-3, an apoptotic cell marker. Of 168,726 cells counted, only 23 cells with activated caspase3 immune reactivity were detected in the p73DD(wt)-treated hearts. Similar rate of program cell death was found in both untreated control and p73DD(mut) hearts (Tab. 2; Fig. 10: D-F).

#### 4.5.5 mRNA and protein expression of cell cycle related genes after directed expression of p73DD(wt)

As mentioned before, mammalian cell cycle progression is especially driven by the regulated activation of various cyclins and cyclin dependent kinases. Since directed expression of p73DD(wt) leads to S- and M-phase entry of cardiomyocytes, further experiments were designed to investigate whether this phenomenon was achieved by a direct transcriptional activation of cyclins, or/and by suppression of inhibitory CKIs.

**Table 4:** Quantitative mRNA expression of cell cycle related genes 14 days after intrathoracic injection of the indicated adenoviruses (n = 4 per group). Data are presented as copy number per 1000 copies GAPDH and as percent of untreated control [86].

Gene	Control	p73DD(wt)	p73DD(mut)
p21WAF	4.1 (100%)	1.9 (46%)	3.8 (94%)
cyclin A	0.79 (100%)	2.06 (263%)	0.97 (124%)
cyclin B1	0.22 (100%)	0.39 (176%)	0.05 (25%)
cyclin B2	1.37 (100%)	4.44 (325%)	1.35 (99%)
cyclin D1	0.25 (100%)	0.25 (101%)	0.23 (94%)
cyclin D2	3.2 (100%)	7.52 (235%)	5.64 (176%)
cyclin D3	8.79 (100%)	9.5 (106%)	5.18 (58%)
cyclin E	0.25 (100%)	0.4 (157%)	0.16 (61%)

As seen in Tab. 4, expression of p73DD(wt) led to a change in the mRNA levels of several cell cycle related genes while the expression of mutant p73DD did not differ from untreated controls in most cases. In particular, p73DD(wt)-induced up-regulation of cyclins that are related to G1/S-transition (cyclin D2), S-phase progression (cyclin A/E) as well as M-phase entry (cyclin B1/B2). Additionally, the mRNA expression of

the cyclin kinase inhibitor p21WAF was significantly reduced after p73DD(wt) injection.

Since changes in mRNA levels do not always lead to changes in corresponding protein levels, key components of the cell cycle machinery were also quantified by Western blot analysis. Accordingly, the majority of genes which were induced by p73DD(wt) on mRNA level also showed increased protein expression. However, the G1/S transition related cyclin D2, which expression was induced by both wildtype and mutant p73DD, showed no difference at the level of protein translation in comparison to untreated control hearts. The transcriptional downregulation of p21WAF after p73DD(wt) expression was confirmed by lower levels of the corresponding protein as well (Fig. 12).

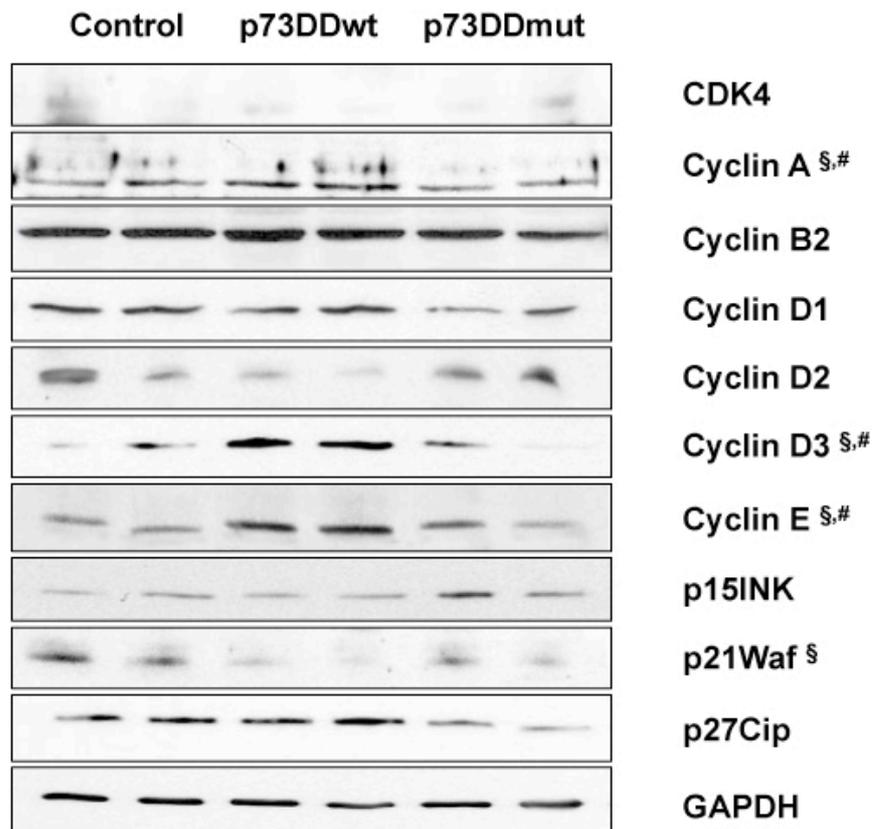


**Figure 12: Western blot analysis of important cell cycle regulators in hearts at day 14 after intrathoracic injection of the indicated adenoviruses (n=4 per group). §p<0.05 vs. control; #p<0.05 vs. p73DD(mut)**

#### 4.6 Effects of directed expression of p73DD(wt) in adult mouse myocardium

The potential of cardiomyocytes to proliferate during embryonic development drops in the perinatal period. This phenomenon raises the question whether the elevated rate of cardiomyocyte proliferation in neonatal mice after p73DD(wt) injection was due to an inhibition or delay of cell cycle arrest rather than to a real induction of cell cycle re-entry. Thus, it should be analyzed next whether expression of the dominant-negative p73DD(wt) does also induce S-phase entry of adult cardiomyocytes.

The recombinant adenoviruses encoding the p73DD-isoforms were directly injected into the myocardium of the left ventricle in adult mice. As the adenoviral constructs also contain the EGFP-cDNA (see material section; 3.1.2), the expression of the recombinant proteins could be directly confirmed on histological sections by analysing EGFP-fluorescence (Fig. 13).

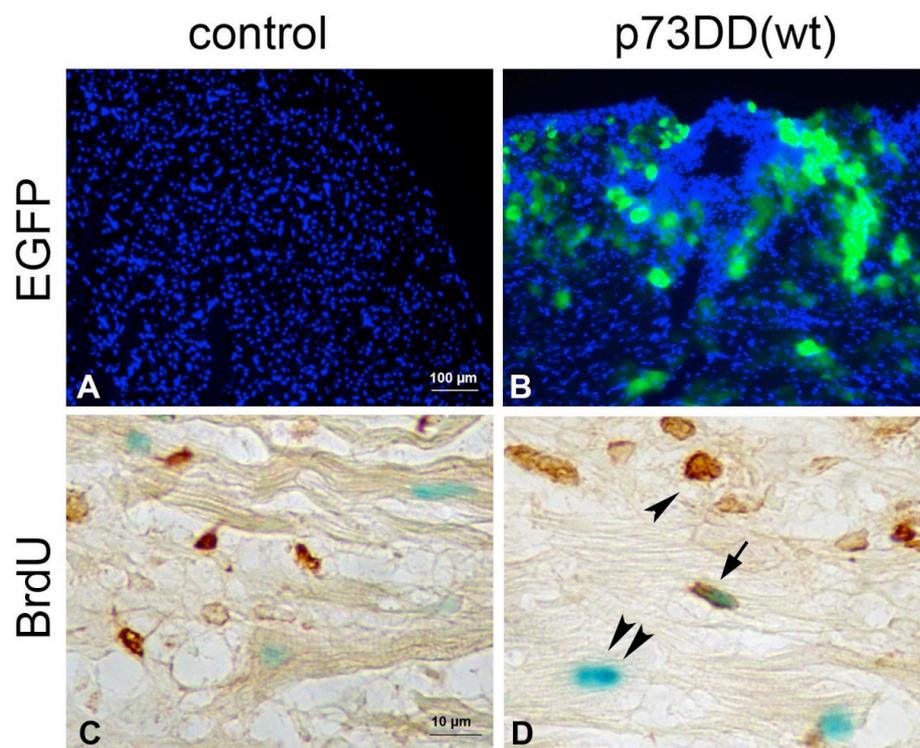


**Figure 13: Histological examples of intramyocardial adenovirus injection in adult mice.**

A+B: EGFP expression (slides were counterstained with the nuclear dyeHoechst33258). C+D: anti-BrdU immunoassay. BrdU-positive adult cardiomyocytes were detected after directed expression of p73DDwt. Arrow: BrdU-positive cardiomyocyte; Single arrowhead: BrdU-positive non-cardiomyocyte; Double arrowhead: BrdU-negative cardiomyocyte.

Cardiomyocytes adjacent to the injection sites were counted for the analysis of cell cycle activity and apoptosis. Interestingly, injection of p73DD(wt) into the myocardium of adult mice also led to a significant elevated rate of cardiomyocyte BrdU-incorporation (Fig. 13). In addition, also an increase of the number of phosphoH3-positive cardiomyocytes after expression of p73DD(wt) was observed although this elevation did not reach statistical significance. In line with the findings in neonatal hearts, no difference was noted regarding the rate of apoptosis between p73DD-injected and untreated control hearts (Tab. 5).

**Table 5:** Parameters of cell cycle activity and apoptosis after directed intramyocardial injection of p73DD(wt) in adult mouse heart (kindly provided by K. Köhler, Universitätsklinik und Poliklinik für Innere Medizin III, Halle (Saale)) [86].

<b>Group</b>	<b>BrdU-positive CM</b>	<b>PhosphoH3-positive CM</b>	<b>Activated caspase3-positive cells</b>
Control (n=6)	6/97830 (0.006%)	2/88675 (0.003%)	2/148293
p73DD(wt) (n=5)	25/106,811 (0.023%) <sup>§</sup>	8/104740 (0.008%)	0/265949

<sup>§</sup>p<0.05 vs control

## 5 DISCUSSION

Coronary artery occlusion attributable to plaque rupture as seen in myocardial infarction results in the death of significant numbers of cardiac myocytes, causing impairment in cardiac function and ultimately often resulting in heart failure. Current therapies can only slow down the progression of patients with heart failure but do not tackle the fundamental problem, i.e., the progressive loss of functional heart muscles. Thus, novel therapeutic strategies aimed at replacing dead or damaged cardiomyocytes would certainly herald a new era of chronic heart failure treatment. A recent explosion of studies using cell transplantations of for example muscle progenitor cells or adult stem cells show some promise in this regard [87]. However, it is currently unclear whether the benefit, mode of action, and the potential side effects of stem cell transplantations will justify a broad clinical application. An alternative approach to replace damaged cardiomyocytes might be the strategy to stimulate the proliferation of remaining cardiomyocytes [88, 89]. Such a strategy would be particularly useful in situations of localized myocardial damage as, e.g., after myocardial infarction.

### 5.1 p73DD(wt) inhibits p53/p73-dependent signaling in vitro

p53 is known to function as a tetramer, and oligomerization of four identical p53 monomers allows its nuclear translocation, where p53 activates its downstream genes by binding to the target response element (RE) sequences [90]. Due to the homologous structure of p53 and p73 proteins, it is generally believed that p73 is also able to bind to these RE [51]. Data from the original study, where the p73DD(wt) was first constructed and used, demonstrates that p73DD(wt) is able to bind to p73 and blocks sequence-specific DNA binding by p73 [52]. This finding was confirmed in the luciferase reporter assay using p53-knockout cell line (H1299) where activation of RE solely depends on p73. However, further analysis presented here using HEK293 cell line suggested that p73DD(wt) interacts with both p53 and p73 thereby inhibits their transcriptional activities, although the authors of the original paper mentioned above stated that p73DD(wt) only binds to p73, but not to p53 [52]. Our view was further supported by the fact that the protein expression of p53 was significantly increased after p73DD(wt)-treatment, indicating the activation of a compensatory feed-back loop which was likely due to the functional abrogation of p53. In addition, a previous study had demonstrated

that another truncated isoform of p73 ( $\Delta$ N-p73) can bind to p53 protein, which markedly suppressed p53-mediated apoptosis in sympathetic neurons in response to nerve growth factor withdrawal [55]. Collectively, the present data suggests that p73DD(wt) functionally abrogates the action of p53/p73-signaling by exerting dominant-negative effects which might be achieved through its integration into tetramers, thereby resulting in the inactivation of endogenous protein activity and the suppression of p53/p73 transcriptional activity.

## **5.2 p73DD(wt) expression promotes cardiomyocyte proliferation in vivo**

Since activation of p53 is known to be a crucial event during the cell cycle exit of cardiomyocytes in the perinatal period [31, 91] and p73DD(wt) was shown to interfere with p53/p73-signaling in cell culture experiments, it seemed possible that expression of p73DD(wt) in neonatal hearts would relax the otherwise stringent regulation of cardiomyocyte cell cycle reentry.

By using aMHC-LacZ transgenic mice, we were able to detect a BrdU-labeling index of 0.67 % in control hearts at an early developmental stage (day 3). The BrdU-labeling index, however, dropped to 0.001 % at day 14 after birth. It is generally believed that cardiac mass increases during fetal life as a consequence of cardiomyocyte proliferation [24, 92]. During neonatal life, a transition from hyperplastic to hypertrophic cardiac growth occurs, which is accompanied by increased numbers of binucleated cardiomyocytes [22]. Therefore, it was not surprising to find a higher BrdU-labeling index at the early developmental stage (day 3) than in later life. Further cell cycle profile analysis, including phosphorylation of histon3 (marker of metaphase; 0 % in control hearts) and AuroraB (marker of cytokinesis; 0 % in control hearts) strongly supported the generally accepted concept [93, 94] that the vast majority of cardiomyocytes lose the ability of proliferation after birth.

It is important to note that cardiomyocytes constitute only 20-30 % of the total number of cells present in the heart and consequently, the preponderance of nuclei present in histological sections of hearts are from non-cardiomyocytes [95]. Thus, assessment of cardiomyocyte DNA synthesis can only be as accurate as the assay used to distinguish cardiomyocyte nuclei from non-myocyte nuclei [22]. In our study, we have used transgenic reporter mice in which the nuclei of all cardiomyocytes are labelled by the LacZ gene (aMHC-nlsLacZ). Thus, we were able to unequivocally differentiate

between cardiomyocytes and non-cardiomyocytes on histological sections, which is indispensable to enable a reliable analysis of the cardiomyocyte cell cycle activity. It is of interest to note that we detected a similar percentage of cardiomyocytes which were in or have passed through S-phase in control samples (control: 0.001 % at day 14; 0.006 % in adult heart) as the group of L. J. Field who has established this transgenic mouse strain (0.003 % in adult heart) [22]. Controversial rates of cardiomyocyte DNA-synthesis were also reviewed in previous studies, where some research groups reported as high as 2 % of mitotic index at day 14 [96]. However, it has to be kept in mind that some of the studies relied on less strict histological methods to identify cardiomyocytes [97], which of course could artificially increase the rate of mitotic index when proliferating non-myocytes are mis-classified [98].

In comparison to control hearts, a strong effect of p73DD(wt) on induction of S-phase entry and mitosis in hearts of newborn mice was observed in the study presented here. This was indicated by a significantly increased rate of BrdU-incorporation, as well as expression of phosphorylated histone H3 and AuroraB in cardiomyocytes, which was found both at day 3 and day 14 after birth. Expression of a control virus, which encodes a mutant p73DD harbouring a point mutation that blocks the dominant-negative property of p73DD(wt), only had little effect on cardiomyocyte cell cycle activity indicating that the effects of p73DD are mediated by interference with p53/p73-signaling and are not due to other unspecific effects.

The observed S-phase entry of adult cardiomyocytes further suggested that cardiomyocyte cell cycle relaxation after p73DD(wt) expression was achieved by an induction of cell cycle re-entry, and not solely by an inhibition or delay of the naturally occurring cell cycle arrest in perinatal life [98]. However, unlike seen for cardiomyocyte DNA synthesis (BrdU-uptake), the extend of mitotic activity (phosphoH3) found after expression of p73DD(wt) in adult heart muscle cells did not reach statistical significance. It seems rather plausible that this is a consequence of differences in the sensitivity of the assays used. As cell that passed S-phase will be permanently marked by BrdU, therefore, BrdU immunoassay is known to stain all cells that underwent S-phase during the time of BrdU-labeling (48 hours in the experiments presented here). In contrast, the phosphorylated H3 immunoassay only detects the cells that are currently in M-phase at the time of tissue fixation [98]. Furthermore, intramyocardial virus injection is of limited efficiency in adult animals so that a better

research model, e.g. aMHC-p73DD(wt) transgenic mice, should be used to further investigate the effects of p73DD(wt) in adulthood in future experiments.

The CDK-inhibitor (CKI) p21WAF which is known to be one of the direct targets of p53, has been shown to severely suppress cell cycle progression of cardiomyocytes [99, 100]. p21WAF was implicated as a key cell cycle regulator, and its dissociation from the CDK complexes led to the activation of CDK2, CDK4 and CDK6 and S-phase reentry of cardiomyocytes followed by the E2F-1 overexpression in the presence of insulin-like growth factor I (IGF-I) [101]. Moreover, a previous study suggested that p21 regulates the proliferating cell nuclear antigen (PCNA) in adult cardiomyocytes, which is essential for DNA-synthesis [100, 102]. As p73DD(wt) functions by interfering with the expression of p53- and p73-dependent genes, it seemed likely that p73DD would have impact on p21WAF expression. Subsequent analysis at the molecular level indeed showed that directed expression of p73DD(wt) strongly inhibited p21WAF mRNA and protein expression, which might in part offer an important mechanism of cardiomyocyte cell cycle relaxation in the presented study [86].

As mentioned before, regulation of cell cycle activity depends on the coordinated action of numerous genes including several cyclins [8]. Previous studies had demonstrated that targeted expression of cyclin A or cyclin D2 in transgenic mice leads to cardiomyocyte proliferation [88, 103]. In our experiments we found an mRNA induction of cyclin A, E, B1, and B2 expression upon directed expression of p73DD(wt), which finally resulted in increased protein levels as revealed by Western blots. Although a high mRNA expression of cyclin D2 was observed after p73DD(wt)-injection, its protein amount was obviously unchanged that perhaps was caused by post-translational modifications. Indeed, increased mRNA expression of cyclin D2 was noted after p73DD(mut) so that the unspecific effects resulting from the p73DD constructs could not be ruled out here. In addition, it is also important to note that the current study does not allow to distinguish whether these cyclins were directly induced by p73DD(wt) or whether their elevation rather reflected the regular course of cell cycle progression and was caused by indirect means [86].

### 5.3 p73DD(wt) induces cardiac hypertrophy in vivo

In the current experiments, it was shown that at early postnatal stage (day 3), expression of p73DD(wt) leads to hyperplastic rather than hypertrophic cardiac cell growth. This was indicated by an increased rate of BrdU-positive cardiomyocytes and a concomitant reduced cell size in comparison to untreated control hearts. The situation obviously changed at day 14, where the mean cell size of cardiomyocytes was significantly increased in p73DD(wt)-treated hearts. It is reasonable to assume that arrest of cell cycle progression of cardiomyocytes, which becomes more fixed in the first 2 weeks after birth, caused a shift from hyperplastic to hypertrophic cell growth. This finding is consistent with previous reports demonstrating that the targeted expression of other cell cycle activators like D-type cyclins in terminally differentiated cardiomyocytes often leads to induction of hypertrophy rather than to proliferation [104].

One possible mechanism to explain the observed hypertrophy is the elevated p300 transcriptional activity found by microarray analysis. p300 is a critical histone acyltransferase (HAT) in muscle that modifies chromatin and associated transcription factors and promotes gene activation [105]. Recent studies have demonstrated that p300 transcriptional activity is enhanced during agonist-induced cardiac hypertrophy and that subsequent blocking of p300-HAT activity inhibits agonist-mediated cardiac growth [76, 106]. Moreover, transgenic mice that overexpress p300 in the heart develop cardiac hypertrophy and eventual heart failure [107]. Importantly, it has been shown that p300 cooperates with p53 in the regulation of p53-mediated transcriptional activity [108]. Thus, it is plausible to presume that functional abrogation of p53 after directed expression of p73DD(wt) leads to activation of a compensatory feedback loop of p300, which subsequently might induce hypertrophic cell growth.

Further analysis of the mode of p73DD(wt)-induced hypertrophy (performed in addition to the experiments presented here [86]) revealed the expression of BNP,  $\beta$ -MHC, and increased deposition of interstitial collagen, which are linked to “pathological” cell growth. Historically, the term “pathological” hypertrophy was introduced to describe a pattern of mal-adaptation of adult cardiomyocytes caused by increased stress. From the molecular point of view, this process is characterized by the re-induction of fetal genes (e.g.  $\beta$ -MHC), which substitute for the mature isoform (e.g.  $\alpha$ -MHC). Using microarray hybridization and real-time PCR it could be demonstrated that expression of p73DD(wt) delays the transition from the proliferating phenotype of fetal cells to

mature “terminally differentiated” cardiomyocytes [86]. It is tempting to speculate that extension of the phase of embryonic gene expression caused by p73DD(wt) collides with the endogenous program of cardiomyocyte maturation thereby enhancing increased maladaptive (-like) cell growth.

#### **5.4 p73DD(wt) expression does not induce cardiomyocyte apoptosis in vivo**

Forced expression of certain oncogenes in cardiomyocytes, such as E1A and E2F1, also induces apoptosis in parallel with proliferation [109, 110]. In particular, p53 is a well-known tumour suppressor that triggers cellular suicide upon various pathological stimuli through transcriptional activation of its downstream pro-apoptotic targets (review in [111]). In the current study, however, no signs of apoptosis induction were seen after directed expression of p73DD(wt) in neonatal as well as in adult hearts. This was provided by the facts that: (i) induction of caspase gene expression was not noted 7 days after p73DD(wt) expression (microarray analysis), and (ii) the rate of activated caspase3-positive cells in neonatal and adult hearts was similar between p73DD(wt), control and p73DD(mut) group (activated caspase3 immunoassay).

#### **5.5 p73DD(wt) and E2Fs**

A large body of evidence indicates that there is extensive crosstalk between the E2F transcription factors and the p53 protein family [112-114]. E2Fs are essential transcriptional factors that induce expression of genes required for the induction of cell cycle entry [4]. Furthermore, p73 was shown to mediate E2F1-induced apoptosis in the absence of p53 [115]. On the other hand, inhibition of the p53-dependent cell cycle inhibitor p21WAF activates cyclin/CDK complexes, which release E2F transcription factors through phosphorylation of retinoblastoma protein (Rb) [116, 117].

Unexpectedly, in the experiments presented here expression of p73DD(wt) had almost no impact on E2F transcription factors according to the microarray analysis, although expression of p73DD(wt) was shown to suppress p53/p73-signaling and inhibited transcription and translation of p21WAF in the neonatal hearts. As a matter of fact, there was also no detectable increase of expression of CDK4 and cyclinD1/D2 on protein level, which somewhat is in line with the unchanged E2F expression. However, it is of importance to note that E2F expression was determined solely by microarray

analysis in this study. Further analysis using quantitative real-time PCR or Western blot would certainly yield further insights into the crosstalk of p53/p73 and E2F-activity but was beyond the scope of the presented work.

### **5.6 p73DD: the “big brother” of dominant-negative p53-isoforms?**

According to a previous study, expression of a dominant-interfering p53 isoform in a transgenic model did not lead to cardiomyocyte proliferation under baseline conditions [32]. In contrast, the present data shows that injection of p73DD(wt) leads to S-phase entry of both neonatal and adult cardiomyocytes. This finding raises the question whether p73DD(wt) acts as a stronger antagonist of cell cycle arrest than the dominant-negative CB7 allele of p53 used previously [32] so that no additional stimuli were necessary to induce cell cycle re-entry.

Although p73 belongs to the p53 family, p73 is nevertheless also able to bind DNA and activate transcription via response elements slightly different from p53RE and hence might affect genes which do not respond to p53 although both p53 and p73 are able to act via the p53 response element (p53RE) [51, 58]. Unfortunately, no data regarding cardiomyocyte cell cycle activity at early developmental stages were reported after the targeted expression of the dominant-interfering p53 isoform mentioned above [32]. Therefore, the possibility that the dominant-interfering p53 isoform is also able to induce cell cycle progression at least shortly after birth cannot be ruled out at present [86].

Moreover, in the present study, the expression of p73DD in adult hearts was achieved by direct intramyocardial injection of the adenoviruses, which also generates an environment of myocardial injury that might stimulate regenerative processes although the presence of cardiomyocytes that incorporated BrdU was not strictly confined to the injection site.

Thus, further experiments using transgenic mice, in which targeted expression of p73DD(wt) in cardiomyocytes, could allow us to directly compare the effects of dominant-interfering p53 and p73 isoforms on cardiac regeneration.

### **5.7 Controversial effects from p73DD(wt) and p73DD(mut) treated hearts**

It was clearly demonstrated in our study that expression of p73DD(wt) has a strong impact on gene expression and cell cycle regulation of cardiomyocytes. Surprisingly, there was also a similar tendency after the expression of the mutant p73DD isoform in some of the assays although p73DD(mut) should not interact with p53 or p73. One possible explanation of this finding might be due to a residual binding activity of mutant p73DD, which might cause a mild inhibition of p53/p73. However, the possibility that the p73DD-isoforms exert other activities in addition to the inhibition of p53/p73 cannot be excluded completely.

### **5.8 Perspectives**

So far, we have to point out that the degree of proliferation of cardiomyocytes, which was achieved by manipulation of the p73/p53 pathway, was relatively low. The plasmids encoding p73DD which were employed for the generation of the recombinant adenoviruses used in this study, were originally used in experiments to explore and suppress the pro-apoptotic mechanisms of E2F1 [52]. In agreement with this study we did not detect an increase in the rate of apoptosis after forced expression of p73DD. Since overexpression of E2F does also stimulate cell cycle entry of cardiomyocytes but often coincides with induction of apoptosis, it seems promising to combine p73DD(wt) and E2Fs to achieve synergistic effects on cardiomyocyte proliferation and heart regeneration in further experiments [89].

Additionally, it will be interesting to investigate whether the ability to undergo proliferation might be reached by any given cardiomyocyte after appropriate cellular reprogramming or resides only in a rare (sub)- population of (stem-cell like) cardiomyocytes.

## 6 CONCLUSION

The current study shows that directed expression of a dominant-negative isoform of p73 (p73DD(wt)) enables cardiomyocytes to re-enter the cell cycle both at neonatal and adult stages. In parallel, p73DD leads to hypertrophic growth without provoking apoptosis. Cell cycle activation in cardiomyocytes seems to be mediated by inhibition of the cdk-inhibitor p21WAF and the induction and stabilization of S- and M-phase cyclins. However, prospective investigations are still mandatory to further explore the potential of p73DD as a candidate to be used for the stimulation of cardiac regeneration.

## 7 REFERENCES

1. Sclafani, R.A. and T.M. Holzen, (2007) Cell cycle regulation of DNA replication. *Annu Rev Genet.* 41:237-80.
2. Blow, J.J., *Eukaryotic DNA replication*. Frontiers in molecular biology 1996, Oxford ; New York: IRL Press. xix, 232 p.
3. Dynlacht, B.D., (1997) Regulation of transcription by proteins that control the cell cycle. *Nature.* 389:149-52.
4. Trimarchi, J.M. and J.A. Lees, (2002) Sibling rivalry in the E2F family. *Nat Rev Mol Cell Biol.* 3:11-20.
5. Murray, A.W., (1992) Creative blocks: cell-cycle checkpoints and feedback controls. *Nature.* 359:599-604.
6. Li, L. and National Institutes of Health (U.S.). DNA Repair Interest Group., *DNA damage cell cycle checkpoint beyond buying time for repair*, 2003, National Institutes of Health: Bethesda, Md.
7. Morgan, D.O., (1995) Principles of CDK regulation. *Nature.* 374:131-4.
8. Grana, X. and E.P. Reddy, (1995) Cell cycle control in mammalian cells: role of cyclins, cyclin dependent kinases (CDKs), growth suppressor genes and cyclin-dependent kinase inhibitors (CKIs). *Oncogene.* 11:211-9.
9. Lew, D.J. and S. Kornbluth, (1996) Regulatory roles of cyclin dependent kinase phosphorylation in cell cycle control. *Curr Opin Cell Biol.* 8:795-804.
10. Millard, S.S. and A. Koff, (1998) Cyclin-dependent kinase inhibitors in restriction point control, genomic stability, and tumorigenesis. *J Cell Biochem Suppl.* 30-31:37-42.
11. Yao, G., T.J. Lee, S. Mori, J.R. Nevins, and L. You, (2008) A bistable Rb-E2F switch underlies the restriction point. *Nat Cell Biol.* 10:476-82.
12. Dou, Q.P., A.H. Levin, S. Zhao, and A.B. Pardee, (1993) Cyclin E and cyclin A as candidates for the restriction point protein. *Cancer Res.* 53:1493-7.
13. Mahbubani, H.M., J.P. Chong, S. Chevalier, P. Thommes, and J.J. Blow, (1997) Cell cycle regulation of the replication licensing system: involvement of a Cdk-dependent inhibitor. *J Cell Biol.* 136:125-35.
14. Li, Y., C.W. Jenkins, M.A. Nichols, and Y. Xiong, (1994) Cell cycle expression and p53 regulation of the cyclin-dependent kinase inhibitor p21. *Oncogene.* 9:2261-8.

15. Toyoshima, H., (1996) [Control of cell cycle by the p27 Cdk-inhibitor]. *Tanpakushitsu Kakusan Koso*. 41:1732-6.
16. Heinen, A., D. Kremer, H.P. Hartung, and P. Kury, (2008) p57 kip2's role beyond Schwann cell cycle control. *Cell Cycle*. 7:2781-6.
17. Iavarone, A. and J. Massague, (1997) Repression of the CDK activator Cdc25A and cell-cycle arrest by cytokine TGF-beta in cells lacking the CDK inhibitor p15. *Nature*. 387:417-22.
18. McConnell, B.B., F.J. Gregory, F.J. Stott, E. Hara, and G. Peters, (1999) Induced expression of p16(INK4a) inhibits both CDK4- and CDK2-associated kinase activity by reassortment of cyclin-CDK-inhibitor complexes. *Mol Cell Biol*. 19:1981-9.
19. Tourigny, M.R., J. Ursini-Siegel, H. Lee, K.M. Toellner, A.F. Cunningham, D.S. Franklin, S. Ely, M. Chen, X.F. Qin, Y. Xiong, I.C. MacLennan, and S. Chen-Kiang, (2002) CDK inhibitor p18(INK4c) is required for the generation of functional plasma cells. *Immunity*. 17:179-89.
20. Cunningham, J.J., E.M. Levine, F. Zindy, O. Goloubeva, M.F. Roussel, and R.J. Smeyne, (2002) The cyclin-dependent kinase inhibitors p19(Ink4d) and p27(Kip1) are coexpressed in select retinal cells and act cooperatively to control cell cycle exit. *Mol Cell Neurosci*. 19:359-74.
21. Pasumarthi, K.B. and L.J. Field, (2002) Cardiomyocyte cell cycle regulation. *Circ Res*. 90:1044-54.
22. Soonpaa, M.H. and L.J. Field, (1998) Survey of studies examining mammalian cardiomyocyte DNA synthesis. *Circ Res*. 83:15-26.
23. Beltrami, A.P., K. Urbanek, J. Kajstura, S.M. Yan, N. Finato, R. Bussani, B. Nadal-Ginard, F. Silvestri, A. Leri, C.A. Beltrami, and P. Anversa, (2001) Evidence that human cardiac myocytes divide after myocardial infarction. *N Engl J Med*. 344:1750-7.
24. Erozhina, I.L., (1968) [The proliferation and DNA synthesis during early stages of myocardial development]. *Tsitologiya*. 10:162-72.
25. Ueno, H., M.B. Perryman, R. Roberts, and M.D. Schneider, (1988) Differentiation of cardiac myocytes after mitogen withdrawal exhibits three sequential states of the ventricular growth response. *J Cell Biol*. 107:1911-8.

26. Soonpaa, M.H., K.K. Kim, L. Pajak, M. Franklin, and L.J. Field, (1996) Cardiomyocyte DNA synthesis and binucleation during murine development. *Am J Physiol.* 271:H2183-9.
27. Clubb, F.J., Jr. and S.P. Bishop, (1984) Formation of binucleated myocardial cells in the neonatal rat. An index for growth hypertrophy. *Lab Invest.* 50:571-7.
28. Vousden, K.H. and D.P. Lane, (2007) p53 in health and disease. *Nat Rev Mol Cell Biol.* 8:275-83.
29. Seoane, J., H.V. Le, and J. Massague, (2002) Myc suppression of the p21(Cip1) Cdk inhibitor influences the outcome of the p53 response to DNA damage. *Nature.* 419:729-34.
30. Esteve, A., T. Lehman, W. Jiang, I.B. Weinstein, C.C. Harris, A. Ruol, A. Peracchia, R. Montesano, and M. Hollstein, (1993) Correlation of p53 mutations with epidermal growth factor receptor overexpression and absence of mdm2 amplification in human esophageal carcinomas. *Mol Carcinog.* 8:306-11.
31. Huh, N.E., K.B. Pasumarthi, M.H. Soonpaa, S. Jing, B. Patton, and L.J. Field, (2001) Functional abrogation of p53 is required for T-Ag induced proliferation in cardiomyocytes. *J Mol Cell Cardiol.* 33:1405-19.
32. Nakajima, H., H.O. Nakajima, S.C. Tsai, and L.J. Field, (2004) Expression of mutant p193 and p53 permits cardiomyocyte cell cycle reentry after myocardial infarction in transgenic mice. *Circ Res.* 94:1606-14.
33. Proskuryakov, S.Y., V.L. Gabai, and A.G. Konoplyannikov, (2002) Necrosis is an active and controlled form of programmed cell death. *Biochemistry (Mosc).* 67:387-408.
34. Majno, G. and I. Joris, (1995) Apoptosis, oncosis, and necrosis. An overview of cell death. *Am J Pathol.* 146:3-15.
35. Lockshin, R.A. and Z. Zakeri, (2002) Caspase-independent cell deaths. *Curr Opin Cell Biol.* 14:727-33.
36. Cook, S.A. and P.A. Poole-Wilson, (1999) Cardiac myocyte apoptosis. *Eur Heart J.* 20:1619-29.
37. Harwood, S.M., M.M. Yaqoob, and D.A. Allen, (2005) Caspase and calpain function in cell death: bridging the gap between apoptosis and necrosis. *Ann Clin Biochem.* 42:415-31.
38. Leist, M. and M. Jaattela, (2001) Four deaths and a funeral: from caspases to alternative mechanisms. *Nat Rev Mol Cell Biol.* 2:589-98.

39. Gupta, S., (2001) Molecular steps of tumor necrosis factor receptor-mediated apoptosis. *Curr Mol Med.* 1:317-24.
40. Nagata, S., (1994) Apoptosis regulated by a death factor and its receptor: Fas ligand and Fas. *Philos Trans R Soc Lond B Biol Sci.* 345:281-7.
41. Nagata, S., (1996) Fas-mediated apoptosis. *Adv Exp Med Biol.* 406:119-24.
42. Fridman, J.S. and S.W. Lowe, (2003) Control of apoptosis by p53. *Oncogene.* 22:9030-40.
43. Mihara, M., S. Erster, A. Zaika, O. Petrenko, T. Chittenden, P. Pancoska, and U.M. Moll, (2003) p53 has a direct apoptogenic role at the mitochondria. *Mol Cell.* 11:577-90.
44. Leibowitz, B. and J. Yu, Mitochondrial signaling in cell death via the Bcl-2 family. *Cancer Biol Ther.* 9:417-22.
45. Ko, L.J. and C. Prives, (1996) p53: puzzle and paradigm. *Genes Dev.* 10:1054-72.
46. Vousden, K.H., (2005) Apoptosis. p53 and PUMA: a deadly duo. *Science.* 309:1685-6.
47. Lane, D.P. and L.V. Crawford, (1979) T antigen is bound to a host protein in SV40-transformed cells. *Nature.* 278:261-3.
48. Hollstein, M., D. Sidransky, B. Vogelstein, and C.C. Harris, (1991) p53 mutations in human cancers. *Science.* 253:49-53.
49. Donehower, L.A., M. Harvey, B.L. Slagle, M.J. McArthur, C.A. Montgomery, Jr., J.S. Butel, and A. Bradley, (1992) Mice deficient for p53 are developmentally normal but susceptible to spontaneous tumours. *Nature.* 356:215-21.
50. Jacks, T., L. Remington, B.O. Williams, E.M. Schmitt, S. Halachmi, R.T. Bronson, and R.A. Weinberg, (1994) Tumor spectrum analysis in p53-mutant mice. *Curr Biol.* 4:1-7.
51. Yang, A. and F. McKeon, (2000) P63 and P73: P53 mimics, menaces and more. *Nat Rev Mol Cell Biol.* 1:199-207.
52. Irwin, M., M.C. Marin, A.C. Phillips, R.S. Seelan, D.I. Smith, W. Liu, E.R. Flores, K.Y. Tsai, T. Jacks, K.H. Vousden, and W.G. Kaelin, Jr., (2000) Role for the p53 homologue p73 in E2F-1-induced apoptosis. *Nature.* 407:645-8.
53. Caput, D., (1997) [P73: a kin to the p52 tumor suppressor gene]. *Bull Cancer.* 84:1081-2.

54. Ikawa, S., A. Nakagawara, and Y. Ikawa, (1999) p53 family genes: structural comparison, expression and mutation. *Cell Death Differ.* 6:1154-61.
55. Pozniak, C.D., S. Radinovic, A. Yang, F. McKeon, D.R. Kaplan, and F.D. Miller, (2000) An anti-apoptotic role for the p53 family member, p73, during developmental neuron death. *Science.* 289:304-6.
56. Yang, A., N. Walker, R. Bronson, M. Kaghad, M. Oosterwegel, J. Bonnin, C. Vagner, H. Bonnet, P. Dikkes, A. Sharpe, F. McKeon, and D. Caput, (2000) p73-deficient mice have neurological, pheromonal and inflammatory defects but lack spontaneous tumours. *Nature.* 404:99-103.
57. Melino, G., V. De Laurenzi, and K.H. Vousden, (2002) p73: Friend or foe in tumorigenesis. *Nat Rev Cancer.* 2:605-15.
58. Sasaki, Y., Y. Naishiro, Y. Oshima, K. Imai, Y. Nakamura, and T. Tokino, (2005) Identification of pigment epithelium-derived factor as a direct target of the p53 family member genes. *Oncogene.* 24:5131-6.
59. Liu, G., S. Nozell, H. Xiao, and X. Chen, (2004) DeltaNp73beta is active in transactivation and growth suppression. *Mol Cell Biol.* 24:487-501.
60. Benard, J., S. Douc-Rasy, and J.C. Ahomadegbe, (2003) TP53 family members and human cancers. *Hum Mutat.* 21:182-91.
61. Melino, G., X. Lu, M. Gasco, T. Crook, and R.A. Knight, (2003) Functional regulation of p73 and p63: development and cancer. *Trends Biochem Sci.* 28:663-70.
62. Murray-Zmijewski, F., D.P. Lane, and J.C. Bourdon, (2006) p53/p63/p73 isoforms: an orchestra of isoforms to harmonise cell differentiation and response to stress. *Cell Death Differ.* 13:962-72.
63. Loiseau, H., J. Arsaut, and J. Demotes-Mainard, (1999) p73 gene transcripts in human brain tumors: overexpression and altered splicing in ependymomas. *Neurosci Lett.* 263:173-6.
64. Donath, M.Y., W. Zierhut, M.A. Gosteli-Peter, C. Hauri, E.R. Froesch, and J. Zapf, (1998) Effects of IGF-I on cardiac growth and expression of mRNAs coding for cardiac proteins after induction of heart hypertrophy in the rat. *Eur J Endocrinol.* 139:109-17.
65. Matsui, T., T. Nagoshi, and A. Rosenzweig, (2003) Akt and PI 3-kinase signaling in cardiomyocyte hypertrophy and survival. *Cell Cycle.* 2:220-3.

66. DeBosch, B., I. Treskov, T.S. Lupu, C. Weinheimer, A. Kovacs, M. Courtois, and A.J. Muslin, (2006) Akt1 is required for physiological cardiac growth. *Circulation*. 113:2097-104.
67. Cho, H., J. Mu, J.K. Kim, J.L. Thorvaldsen, Q. Chu, E.B. Crenshaw, 3rd, K.H. Kaestner, M.S. Bartolomei, G.I. Shulman, and M.J. Birnbaum, (2001) Insulin resistance and a diabetes mellitus-like syndrome in mice lacking the protein kinase Akt2 (PKB beta). *Science*. 292:1728-31.
68. Antos, C.L., T.A. McKinsey, N. Frey, W. Kutschke, J. McAnally, J.M. Shelton, J.A. Richardson, J.A. Hill, and E.N. Olson, (2002) Activated glycogen synthase-3 beta suppresses cardiac hypertrophy in vivo. *Proc Natl Acad Sci U S A*. 99:907-12.
69. Weber, K.T. and C.G. Brilla, (1991) Pathological hypertrophy and cardiac interstitium. Fibrosis and renin-angiotensin-aldosterone system. *Circulation*. 83:1849-65.
70. See, F., A. Kompa, J. Martin, D.A. Lewis, and H. Krum, (2005) Fibrosis as a therapeutic target post-myocardial infarction. *Curr Pharm Des*. 11:477-87.
71. Magnani, B., (2000) [Physiological and pathological cardiac hypertrophy]. *Ital Heart J*. 1 Suppl 2:42-9.
72. van Rooij, E., L.B. Sutherland, J.E. Thatcher, J.M. DiMaio, R.H. Naseem, W.S. Marshall, J.A. Hill, and E.N. Olson, (2008) Dysregulation of microRNAs after myocardial infarction reveals a role of miR-29 in cardiac fibrosis. *Proc Natl Acad Sci U S A*. 105:13027-32.
73. Verdone, L., M. Caserta, and E. Di Mauro, (2005) Role of histone acetylation in the control of gene expression. *Biochem Cell Biol*. 83:344-53.
74. Wood, A. and A. Shilatifard, (2004) Posttranslational modifications of histones by methylation. *Adv Protein Chem*. 67:201-22.
75. Legube, G. and D. Trouche, (2003) Regulating histone acetyltransferases and deacetylases. *EMBO Rep*. 4:944-7.
76. Gusterson, R.J., E. Jazrawi, I.M. Adcock, and D.S. Latchman, (2003) The transcriptional co-activators CREB-binding protein (CBP) and p300 play a critical role in cardiac hypertrophy that is dependent on their histone acetyltransferase activity. *J Biol Chem*. 278:6838-47.
77. Yao, T.P., S.P. Oh, M. Fuchs, N.D. Zhou, L.E. Ch'ng, D. Newsome, R.T. Bronson, E. Li, D.M. Livingston, and R. Eckner, (1998) Gene dosage-dependent

- embryonic development and proliferation defects in mice lacking the transcriptional integrator p300. *Cell*. 93:361-72.
78. McKinsey, T.A. and E.N. Olson, (2004) Dual roles of histone deacetylases in the control of cardiac growth. *Novartis Found Symp.* 259:132-41; discussion 141-5, 163-9.
  79. Haberland, M., R.L. Montgomery, and E.N. Olson, (2009) The many roles of histone deacetylases in development and physiology: implications for disease and therapy. *Nat Rev Genet.* 10:32-42.
  80. Wolff, J.A. and J. Lederberg, (1994) An early history of gene transfer and therapy. *Hum Gene Ther.* 5:469-80.
  81. Schiedner, G., N. Morral, R.J. Parks, Y. Wu, S.C. Koopmans, C. Langston, F.L. Graham, A.L. Beaudet, and S. Kochanek, (1998) Genomic DNA transfer with a high-capacity adenovirus vector results in improved in vivo gene expression and decreased toxicity. *Nat Genet.* 18:180-3.
  82. Ebelt, H. and T. Braun, (2003) Optimized, highly efficient transfer of foreign genes into newborn mouse hearts in vivo. *Biochem Biophys Res Commun.* 310:1111-6.
  83. Nakagawa, T., M. Takahashi, T. Ozaki, K. Watanabe Ki, S. Todo, H. Mizuguchi, T. Hayakawa, and A. Nakagawara, (2002) Autoinhibitory regulation of p73 by Delta Np73 to modulate cell survival and death through a p73-specific target element within the Delta Np73 promoter. *Mol Cell Biol.* 22:2575-85.
  84. Muller-Werdan, U., D. Klein, M. Zander, K. Werdan, and C. Hammer, (1994) Beating neonatal rat cardiomyocytes as a model to study the role of xenoreactive natural antibodies in xenotransplantation. *Transplantation.* 58:1403-9.
  85. Ebelt, H., M. Jungblut, Y. Zhang, T. Kubin, S. Kostin, A. Technau, S. Oustanina, S. Niebrugge, J. Lehmann, K. Werdan, and T. Braun, (2007) Cellular cardiomyoplasty: improvement of left ventricular function correlates with the release of cardioactive cytokines. *Stem Cells.* 25:236-44.
  86. Ebelt, H., Y. Zhang, K. Kohler, J. Xu, P. Gajawada, T. Boettger, T. Hollemann, U. Muller-Werdan, K. Werdan, and T. Braun, (2008) Directed expression of dominant-negative p73 enables proliferation of cardiomyocytes in mice. *J Mol Cell Cardiol.* 45:411-9.
  87. Schachinger, V., B. Assmus, M.B. Britten, J. Honold, R. Lehmann, C. Teupe, N.D. Abolmaali, T.J. Vogl, W.K. Hofmann, H. Martin, S. Dimmeler, and A.M.

- Zeiber, (2004) Transplantation of progenitor cells and regeneration enhancement in acute myocardial infarction: final one-year results of the TOPCARE-AMI Trial. *J Am Coll Cardiol.* 44:1690-9.
88. Pasumarthi, K.B., H. Nakajima, H.O. Nakajima, M.H. Soonpaa, and L.J. Field, (2005) Targeted expression of cyclin D2 results in cardiomyocyte DNA synthesis and infarct regression in transgenic mice. *Circ Res.* 96:110-8.
89. Ebel, H., N. Hufnagel, P. Neuhaus, H. Neuhaus, P. Gajawada, A. Simm, U. Muller-Werdan, K. Werdan, and T. Braun, (2005) Divergent siblings: E2F2 and E2F4 but not E2F1 and E2F3 induce DNA synthesis in cardiomyocytes without activation of apoptosis. *Circ Res.* 96:509-17.
90. Wang, P., M. Reed, Y. Wang, G. Mayr, J.E. Stenger, M.E. Anderson, J.F. Schwedes, and P. Tegtmeier, (1994) p53 domains: structure, oligomerization, and transformation. *Mol Cell Biol.* 14:5182-91.
91. Pasumarthi, K.B., S.C. Tsai, and L.J. Field, (2001) Coexpression of mutant p53 and p193 renders embryonic stem cell-derived cardiomyocytes responsive to the growth-promoting activities of adenoviral E1A. *Circ Res.* 88:1004-11.
92. Erokhina, E.L., (1968) [Proliferation dynamics of cellular elements in the differentiating mouse myocardium]. *Tsitologiya.* 10:1391-409.
93. Rumyantsev, P.P., (1977) Interrelations of the proliferation and differentiation processes during cardiac myogenesis and regeneration. *Int Rev Cytol.* 51:186-273.
94. McGill, C.J. and G. Brooks, (1995) Cell cycle control mechanisms and their role in cardiac growth. *Cardiovasc Res.* 30:557-69.
95. Soonpaa, M.H. and L.J. Field, (1997) Assessment of cardiomyocyte DNA synthesis in normal and injured adult mouse hearts. *Am J Physiol.* 272:H220-6.
96. Machida, N., N. Brissie, C. Sreenan, and S.P. Bishop, (1997) Inhibition of cardiac myocyte division in c-myc transgenic mice. *J Mol Cell Cardiol.* 29:1895-902.
97. Connolly, K.M. and M.S. Bogdanffy, (1993) Evaluation of proliferating cell nuclear antigen (PCNA) as an endogenous marker of cell proliferation in rat liver: a dual-stain comparison with 5-bromo-2'-deoxyuridine. *J Histochem Cytochem.* 41:1-6.
98. Ebel, H., Y. Zhang, A. Kampke, J. Xu, A. Schlitt, M. Buerke, U. Muller-Werdan, K. Werdan, and T. Braun, (2008) E2F2 expression induces

- proliferation of terminally differentiated cardiomyocytes in vivo. *Cardiovasc Res.* 80:219-26.
99. Gottifredi, V., O. Karni-Schmidt, S.S. Shieh, and C. Prives, (2001) p53 down-regulates CHK1 through p21 and the retinoblastoma protein. *Mol Cell Biol.* 21:1066-76.
  100. Engel, F.B., L. Hauck, M. Boehm, E.G. Nabel, R. Dietz, and R. von Harsdorf, (2003) p21(CIP1) Controls proliferating cell nuclear antigen level in adult cardiomyocytes. *Mol Cell Biol.* 23:555-65.
  101. von Harsdorf, R., L. Hauck, F. Mehrhof, U. Wegenka, M.C. Cardoso, and R. Dietz, (1999) E2F-1 overexpression in cardiomyocytes induces downregulation of p21CIP1 and p27KIP1 and release of active cyclin-dependent kinases in the presence of insulin-like growth factor I. *Circ Res.* 85:128-36.
  102. Prelich, G., C.K. Tan, M. Kostura, M.B. Mathews, A.G. So, K.M. Downey, and B. Stillman, (1987) Functional identity of proliferating cell nuclear antigen and a DNA polymerase-delta auxiliary protein. *Nature.* 326:517-20.
  103. Cheng, R.K., T. Asai, H. Tang, N.H. Dashoush, R.J. Kara, K.D. Costa, Y. Naka, E.X. Wu, D.J. Wolgemuth, and H.W. Chaudhry, (2007) Cyclin A2 induces cardiac regeneration after myocardial infarction and prevents heart failure. *Circ Res.* 100:1741-8.
  104. Tamamori-Adachi, M., H. Ito, K. Nobori, K. Hayashida, J. Kawauchi, S. Adachi, M.A. Ikeda, and S. Kitajima, (2002) Expression of cyclin D1 and CDK4 causes hypertrophic growth of cardiomyocytes in culture: a possible implication for cardiac hypertrophy. *Biochem Biophys Res Commun.* 296:274-80.
  105. Olson, E.N., J. Backs, and T.A. McKinsey, (2006) Control of cardiac hypertrophy and heart failure by histone acetylation/deacetylation. *Novartis Found Symp.* 274:3-12; discussion 13-9, 152-5, 272-6.
  106. Yanazume, T., K. Hasegawa, T. Morimoto, T. Kawamura, H. Wada, A. Matsumori, Y. Kawase, M. Hirai, and T. Kita, (2003) Cardiac p300 is involved in myocyte growth with decompensated heart failure. *Mol Cell Biol.* 23:3593-606.
  107. Miyamoto, S., T. Kawamura, T. Morimoto, K. Ono, H. Wada, Y. Kawase, A. Matsumori, R. Nishio, T. Kita, and K. Hasegawa, (2006) Histone acetyltransferase activity of p300 is required for the promotion of left ventricular

- remodeling after myocardial infarction in adult mice in vivo. *Circulation*. 113:679-90.
108. Ito, A., C.H. Lai, X. Zhao, S. Saito, M.H. Hamilton, E. Appella, and T.P. Yao, (2001) p300/CBP-mediated p53 acetylation is commonly induced by p53-activating agents and inhibited by MDM2. *Embo J*. 20:1331-40.
  109. Agah, R., L.A. Kirshenbaum, M. Abdellatif, L.D. Truong, S. Chakraborty, L.H. Michael, and M.D. Schneider, (1997) Adenoviral delivery of E2F-1 directs cell cycle reentry and p53-independent apoptosis in postmitotic adult myocardium in vivo. *J Clin Invest*. 100:2722-8.
  110. Kirshenbaum, L.A. and M.D. Schneider, (1995) Adenovirus E1A represses cardiac gene transcription and reactivates DNA synthesis in ventricular myocytes, via alternative pocket protein- and p300-binding domains. *J Biol Chem*. 270:7791-4.
  111. Schuler, M. and D.R. Green, (2001) Mechanisms of p53-dependent apoptosis. *Biochem Soc Trans*. 29:684-8.
  112. Wu, X. and A.J. Levine, (1994) p53 and E2F-1 cooperate to mediate apoptosis. *Proc Natl Acad Sci U S A*. 91:3602-6.
  113. Lee, C.W., T.S. Sorensen, N. Shikama, and N.B. La Thangue, (1998) Functional interplay between p53 and E2F through co-activator p300. *Oncogene*. 16:2695-710.
  114. Moroni, M.C., E.S. Hickman, E. Lazzerini Denchi, G. Caprara, E. Colli, F. Cecconi, H. Muller, and K. Helin, (2001) Apaf-1 is a transcriptional target for E2F and p53. *Nat Cell Biol*. 3:552-8.
  115. Stiewe, T. and B.M. Putzer, (2000) Role of the p53-homologue p73 in E2F1-induced apoptosis. *Nat Genet*. 26:464-9.
  116. Weinberg, R.A., (1995) The retinoblastoma protein and cell cycle control. *Cell*. 81:323-30.
  117. Hiyama, H., A. Iavarone, and S.A. Reeves, (1998) Regulation of the cdk inhibitor p21 gene during cell cycle progression is under the control of the transcription factor E2F. *Oncogene*. 16:1513-23.

## 8 THESEN

1. Herzmuskelzellen von Säugetieren verlieren in der Perinatalzeit die Fähigkeit zu Proliferation und Zellteilung, so dass der adulte Organismus nicht in der Lage ist, untergegangene Herzmuskelzellen (z.B. nach einem Herzinfarkt) zu ersetzen.
2. In der Vergangenheit konnte gezeigt werden, dass bei der Aufrechterhaltung dieser kardiomyozytären Zellzyklus-Blockade p53 eine wesentliche Rolle spielt. p53 stellt jedoch einen typischen Tumor-Suppressor dar, so dass die p53-Hemmung mit dem Risiko der Tumor-Induktion gebunden ist.
3. p73 stellt ein Mitglied der p53-Familie dar, das in struktureller und funktioneller Hinsicht p53 sehr ähnlich ist. Im Gegensatz zu p53 stellt p73 keinen typischen Tumor-Suppressor im engeren Sinne dar.
4. Mittels rekombinanter Adenoviren wurden die Auswirkungen der gezielten Expression von p73DD – einer trunkierten Version von p73 mit dominant-negativen Eigenschaften gegenüber p73 und p53 – auf Proliferation und Apoptose von neonatalen und adulten Kardiomyozyten analysiert.
5. Es konnte gezeigt werden, dass die Expression von p73DD bei neonatalen Tieren in einem signifikanten Anstieg der relativen Herzgewichte resultiert.
6. Die Auswirkung auf die Zellzyklus-Aktivität der Kardiomyozyten wurden anhand von BrdU-Inkorporation, Phosphorylierung von Histon3 und Expression von AuroraB bestimmt. p73DD führt sowohl in neonatalen als auch in adulten Mäusen zur vermehrten Proliferation von Kardiomyozyten
7. Der Zellzyklus-Eintritt ist nicht von vermehrten Kardiomyozyten-Apoptosen begleitet.
8. Als molekularer Mechanismus der Proliferationssteigerung lässt sich die Inhibierung des bekanntermaßen p53-abhängigen CDK-Inhibitors p21WAF nachweisen.
9. Des Weiteren zeigt sich, dass p73DD auch zur Induktion von D-Cycline, Cyclin A, B2 und E führt.

10. p73DD könnte somit einen versprechenden Kandidaten zur Stimulation der Proliferation von Kardiomyzyten im Rahmen regenerativer Therapieansätze darstellen.

**LEBENS LAUF**

## PERSÖNLICHE ANGABEN

Familienname	ZHANG
Vorname	Ying
Geschlecht	männlich
Geburtsdatum	27. März 1979
Geburtsort	Jiangsu, VR China
E-mail	<a href="mailto:ying.zhang@uk-halle.de">ying.zhang@uk-halle.de</a>

## SCHULAUSSBILDUNG

1985-1991	Grundschule Jiangsu, VR China
1991-1997	Mittelschule und Gymnasium Jiangsu, VR China

## UNIVERSITÄTSAUSBILDUNG

1997-2002	Medizinstudium Zweite Medizinische Hochschule, Shanghai, VR China
2003-2006	Postgraduiertenstudium "Biomedical Engineering" Martin-Luther-Universität Halle-Wittenberg und Hochschule Anhalt Abschluss: Master of Engineering (MEng) in Biomedical Engineering
2006-2011	Promotionsstudium Universitätsklinik und Poliklinik für Innere Medizin III Martin-Luther-Universität Halle-Wittenberg

## BERUFSTÄTIGKEIT

2002-2003	Assistenzarzt an der Abteilung für Anästhesie Achstes Krankenhaus, Schanghai, VR China
-----------	---

2006-2010	Wissenschaftlicher Mitarbeiter an der Universitätsklinik und Poliklinik für Innere Medizin III  Martin-Luther-Universität Halle-Wittenberg
08.2010-	Assistenzarzt an der Universitätsklinik und Poliklinik für Innere Medizin III  Martin-Luther-Universität Halle-Wittenberg

**SELBSTÄNDIGKEITSERKLÄRUNG**

Gemäß §6 der Promotionsordnung der Universität Halle erkläre ich hiermit an Eides statt, dass ich vorliegende Arbeit ohne unzulässige Hilfe Dritter und ohne Benutzung anderer als der angegebenen Hilfsmittel angefertigt habe. Die aus anderen Quellen direkt oder indirect übernommenen Daten und Konzepte sind unter Angabe der Quelle gekennzeichnet. Frühere Promotionsversuche bestehen nicht. Die vorliegende Arbeit wurde weder im Inland noch im Ausland in gleicher oder ähnlicher Form einer anderen Prüfungsbehörde vorgelegt.

Halle (Saale), August 2011

Ying Zhang

## **ACKNOWLEDGMENTS**

My special thanks are given to my supervisor PD. Dr. Henning Ebel for offering me the opportunity to work on this project, which allowed me to start in the very interesting field of modern molecular cardiology. I am very grateful to him for giving patient guidance when I was a beginner, encouraging me to face the challenges, and providing constructive discussion and suggestions throughout this doctoral work.

I express my gratitude to Prof. Dr. Karl Werdan for allowing me to start my doctoral work in the department of internal medicine III at Martin-Luther University, Halle (Saale).

Many thanks are to Nicole Glaubitz for her excellent technical assistance.

Sincerely thanks to Prof. Dr. Thomas Braun for the kind support for the microarray experiment at the Max-Planck-Institute for Heart and Lung Research, Bad Nauheim, Germany.

I am very grateful to my parents, the rest of my family and my wife Jia Xu, for their love, constant support and understanding throughout my master and doctoral study.